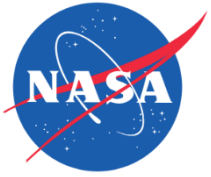


Thermal Vacuum Test Correlation of a Zero Propellant Load Case Thermal Capacitance Propellant Gauging Analytical Model

Stephen A. McKim

**Dept. of Aerospace Engineering; University of Maryland, College Park
Code 597 Propulsion Branch; NASA Goddard Space Flight Center**

**M.S. Aerospace Engineering Thesis Defense
April 6, 2016**



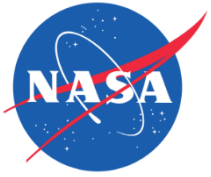
Agenda

- **Introduction**
- **Motivation & Focus**
- **Thesis Objective**
- **Acceptance Criteria**
- **Background**
- **Description of Tank**
- **Theory**
- **Assumptions**
- **Model Development**
- **Correlation Process & Studies**
- **Final Results**
- **Uncertainty Analysis**
- **Conclusion**
- **Future Work**



Introduction

- **Knowledge of remaining propellant is essential to determine the operating life of spacecraft**
- **Instrumentation to gauge propellant is limited**
 - Measurements of temperature & pressure most common
- **Indirect methods must be developed to gauge propellant**
 - Estimate uncertainty important
- **NASA's Magnetospheric Multiscale (MMS) spacecraft is one example that will rely on indirect propellant gauging**
 - Uses a blow-down propulsion system
 - Carries 400 kg of propellant, contained within four propellant tanks



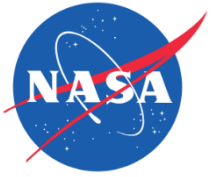
Motivation & Focus

- **Motivation**

- Propellant knowledge important on MMS to:
 - Maintain closely spaced (10 km) formation
 - Change orbit half-way through mission
 - Determine mission length and decommissioning
- Motivates need to develop a propellant load estimator to determine propellant load with low levels of uncertainty

- **Focus**

- Developing and validating thermal model that is foundation of estimator



Thesis Objective

- **Primary Objective:**

- Develop the thermal model of the MMS propellant tank
- Validate model with thermal vacuum test data so that it is sufficient to make future propellant estimates on MMS

- **Secondary Objective:**

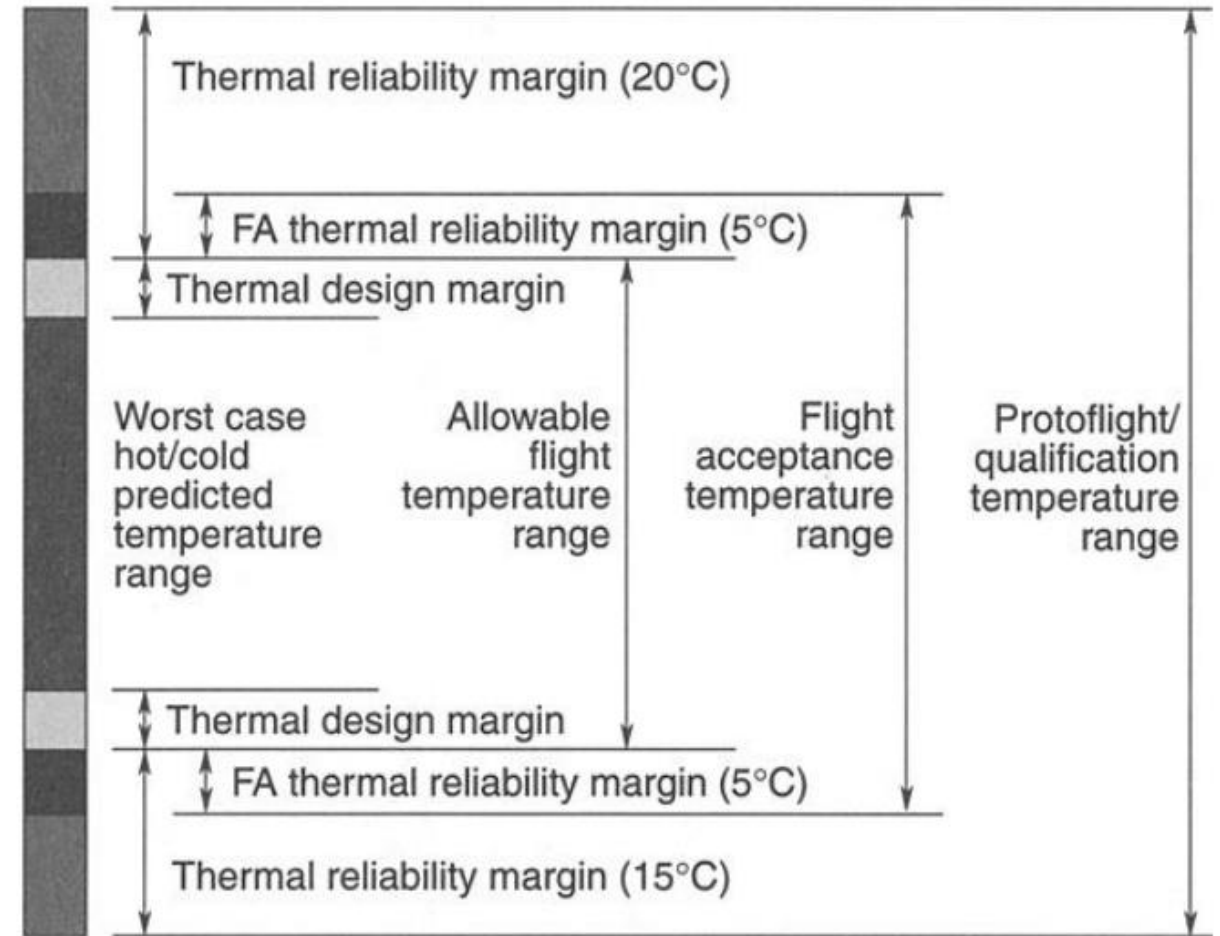
- Provide specifics to create a TCM propellant estimator for diaphragm-style propellant tanks
- Understand process of correlating thermal model to test data

- **Criterion:**

Temperature predictions are within $\pm 3^{\circ}\text{C}$ of the test data at each sensor location

- **Justification:**

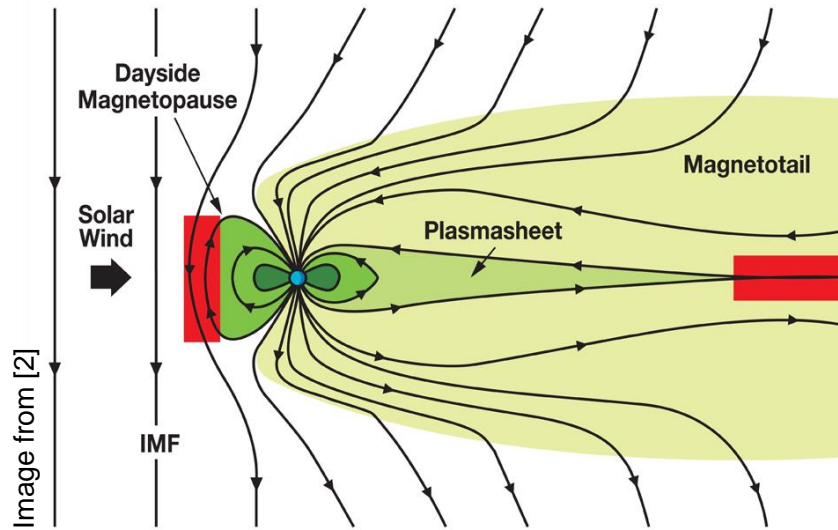
- Criteria is considered industry baseline
- Used by thermal analysts in Thermal Branch at NASA Goddard Space Flight Center
- Within flight acceptance thermal reliability margin of $\pm 5^{\circ}\text{C}$ used by JPL/NASA



Thermal Margins from Gilmore. [1]

Background

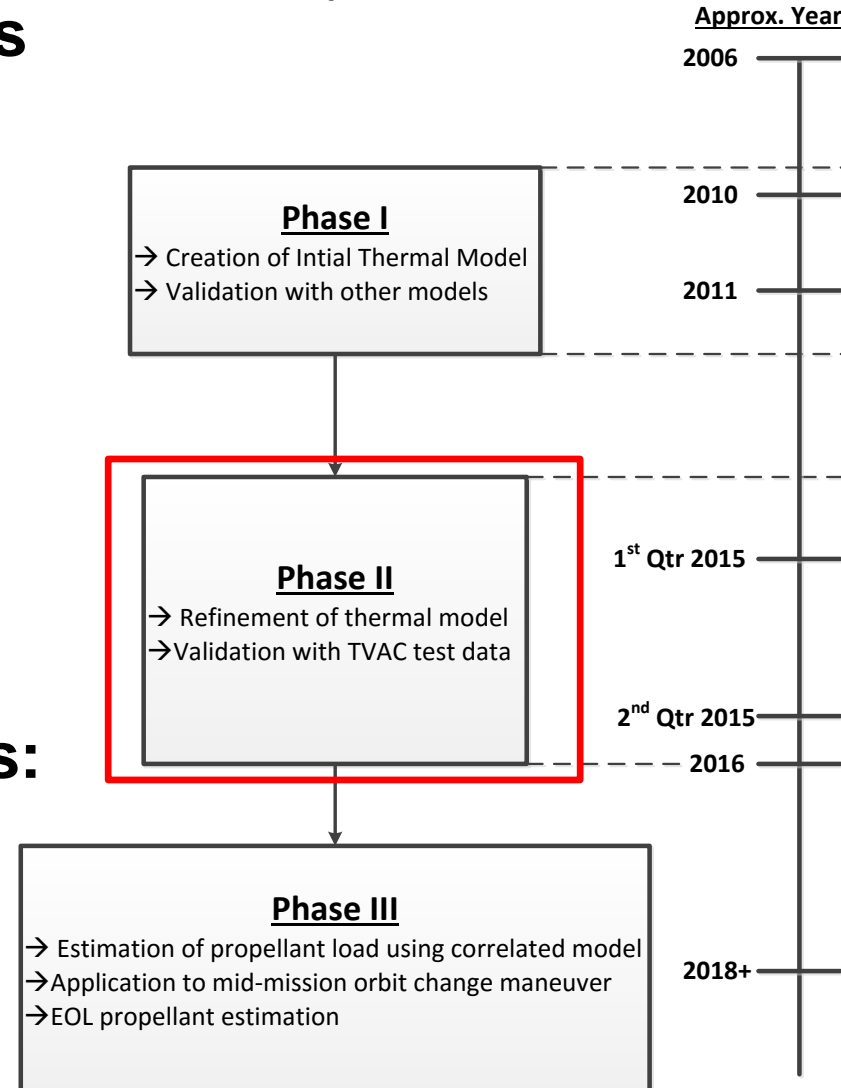
- **Mission goal: understand process of magnetic reconnection**



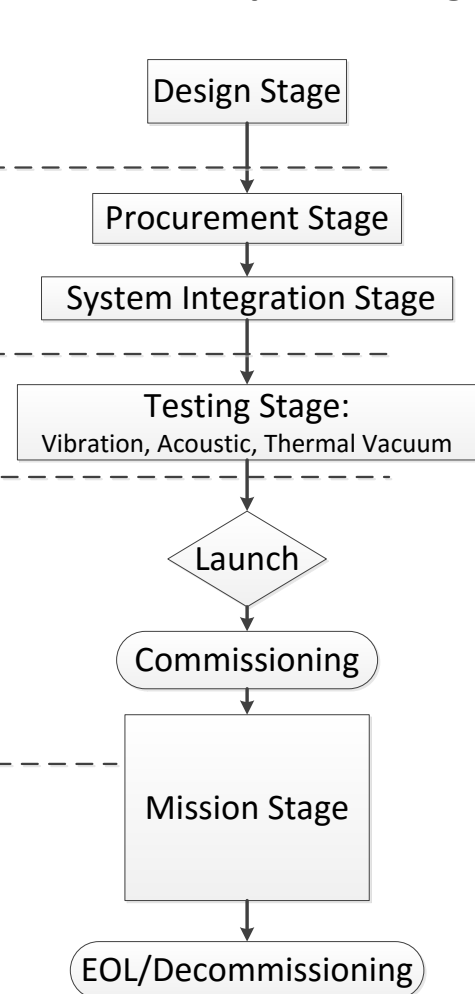
- **Have/will have following data sets:**

- Thermal Vacuum test data
- Commissioning data
- Mid-course correction
- EOL propellant gauging

TCM Development Phase



MMS Development Stage



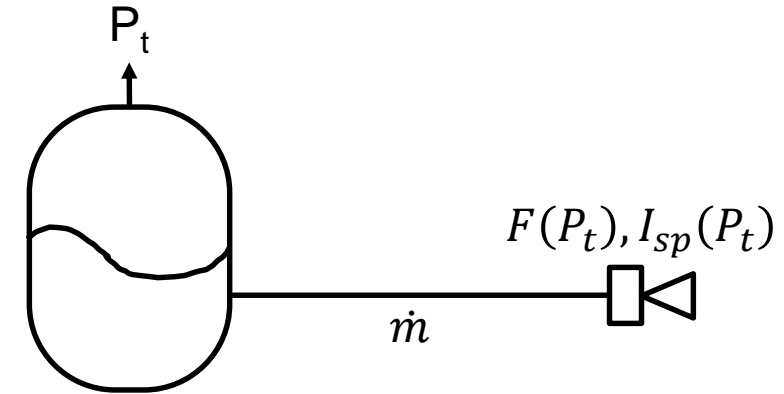
Book Keeping Method (BKM)

- Description:**

- Estimate made from calculated propellant consumption of each maneuver
- Amount of propellant is tabulated for each subsequent maneuver
- F & I_{sp} from test data for each engine

$$\dot{m} = \frac{F(P_t)}{I_{sp}(P_t)}$$

$$m_p = \dot{m} t_m$$



- Advantages:**

- Simple to implement
- Low uncertainty in estimates at the beginning of life

- Disadvantages:**

- Pressure drop and thruster performance models do not account for changes in component performance
- Uncertainty in estimate grows due to compounding of errors
- Estimates of error at end-of-life range widely: 5% to 76%

Pressure-Volume-Temperature Method (PVT)

- **Description:**

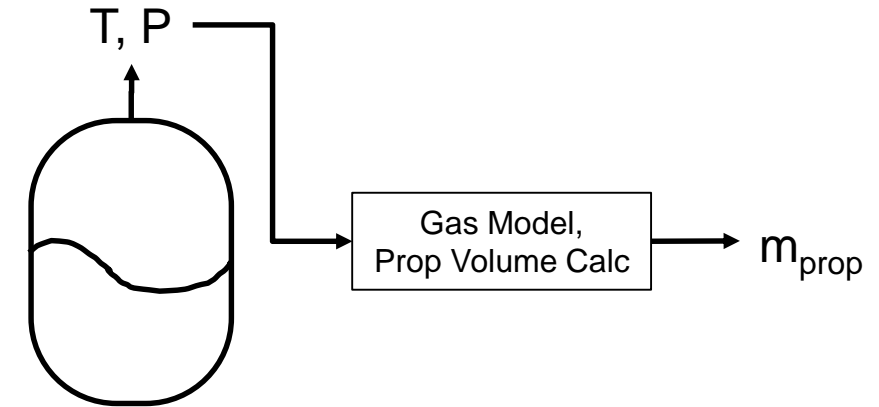
- Estimates from calculating the volume of propellant remaining using real or ideal gas models
- Based upon measured temperature and pressure of the tank
- Independent of previous measurements

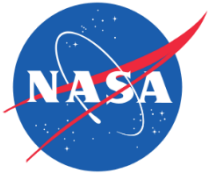
- **Advantages:**

- Accurate at beginning of life
- Estimates independent of previous estimates
- Simple to implement model

- **Disadvantages:**

- Error increases over life of mission due to small changes in pressure compared to change in propellant volume & increased errors in sensor readings
- Highly sensitive to uncertainties in pressure readings
 - Less than 1% uncertainty in pressure reading translates to ~10% or greater in estimated propellant volume





Thermal Capacitance Method (TCM)

- **Description:**

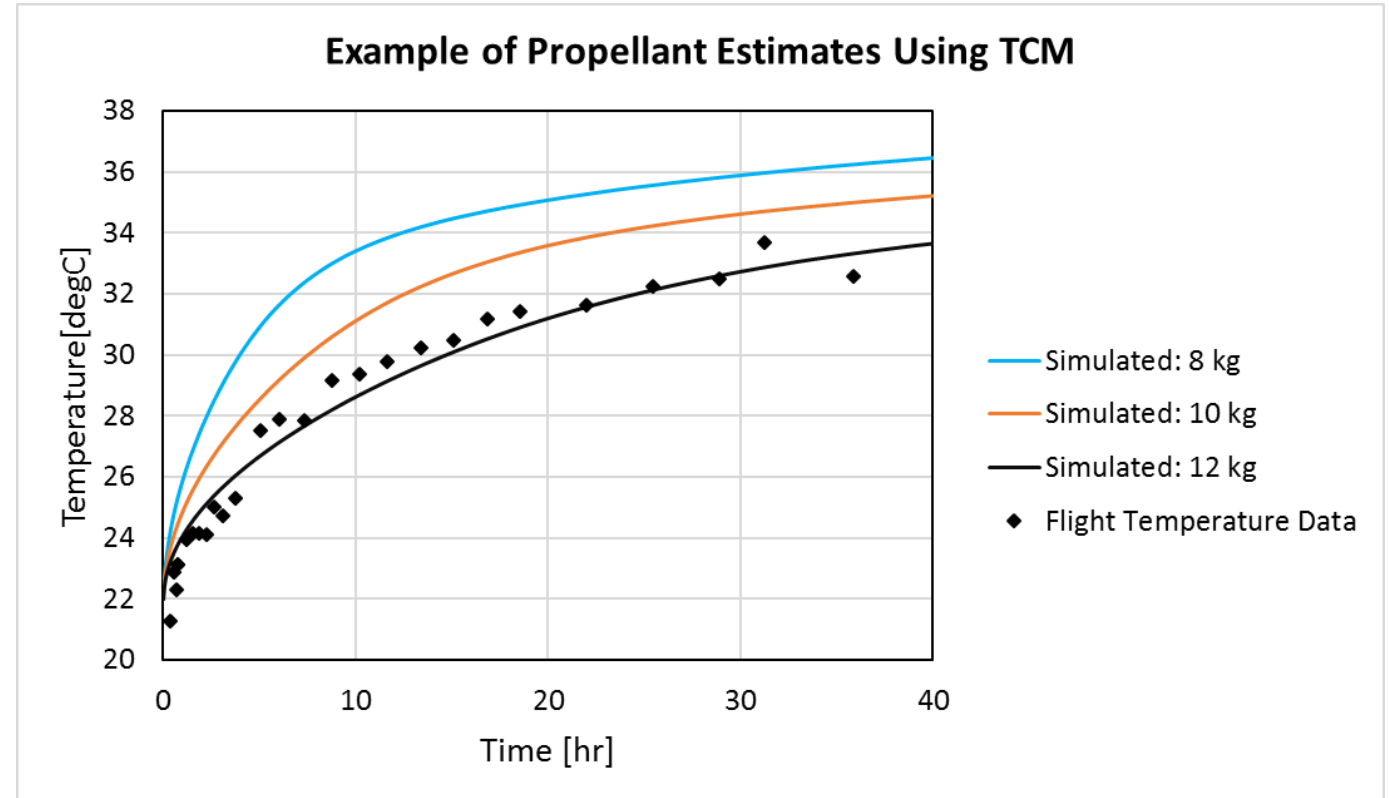
- Propellant estimates based upon temperature response of tank to a known heat input

- **Advantages:**

- Low uncertainties in propellant estimates at end of life
- Less mass leads to higher temperature response which reduces errors

- **Disadvantages:**

- Requires a complex thermal model
- Not accurate at beginning of life due to large propellant mass that reduces the temperature time derivative



Simulated TCM results for different propellant masses are compared to flight telemetry values to obtain a propellant estimate.



Applications of Thermal Capacitance Methods

- **TCM successfully implemented on multiple spacecraft over last 15 years**
- **Publically available reports published through AIAA by Boris Yendler & Co-Authors.**

Spacecraft/System	Year	Ref.
SkyPerfect (JSAT) /Boeing BSS 601 Bus	2007	[3],[4]
Telstar 11	2008	[5]
Turksat 1C/Spacebus 2000	2008	[6]
Arabsat 2B/SpaceBus 3000A	2012	[7]
GEOStar 1A & 1B	2013, 2014	[8],[9]

- **Papers outline highly generalized TCM estimation method**
- **Lack specifics about practical implementation of method**

How do we model the system?

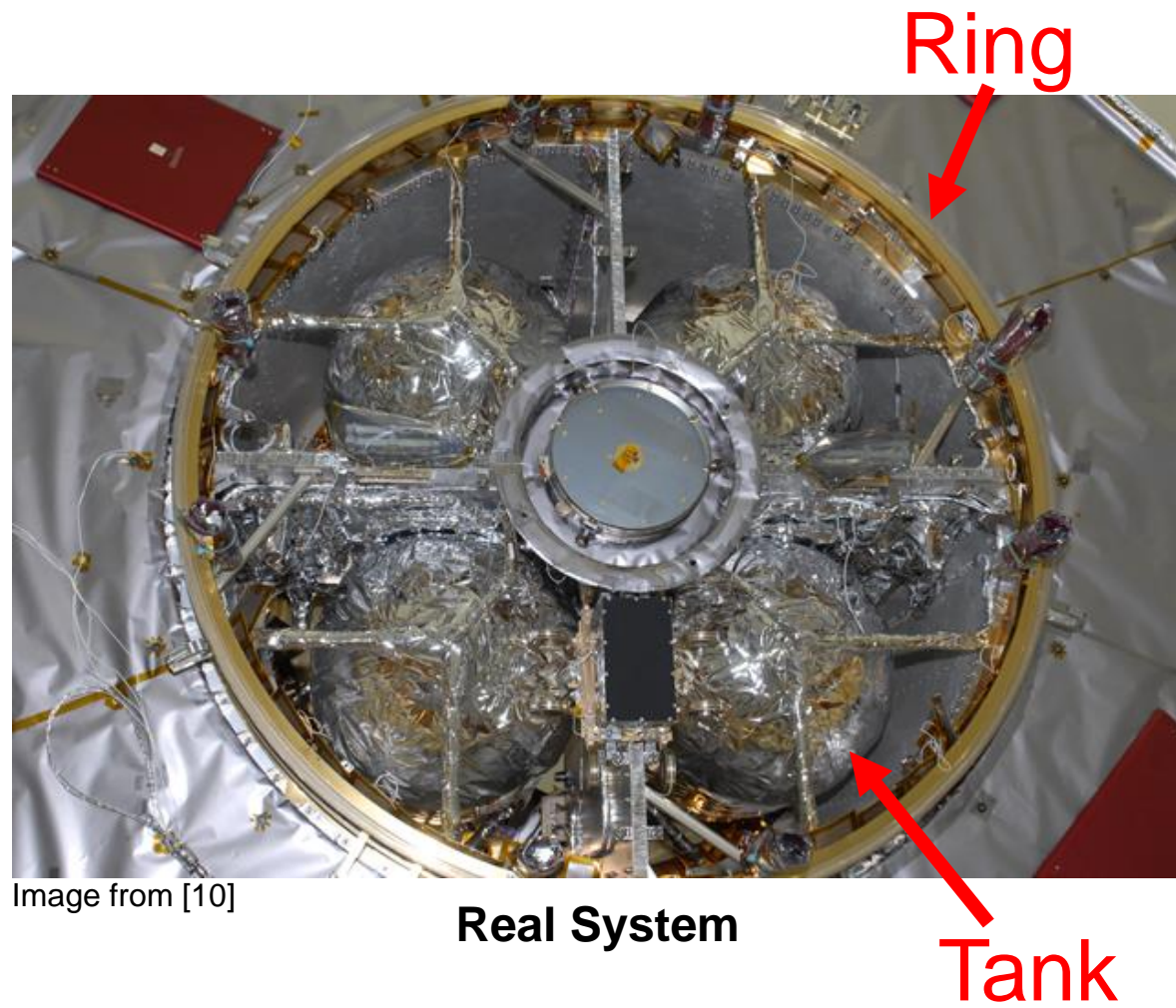
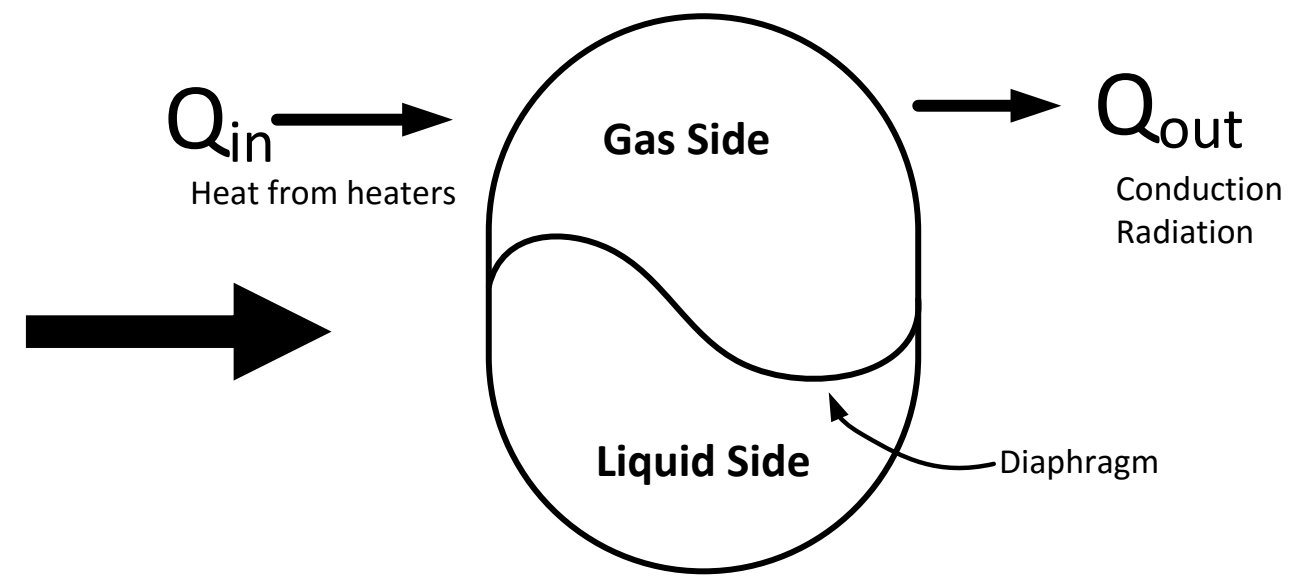
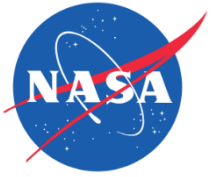


Image from [10]

Real System

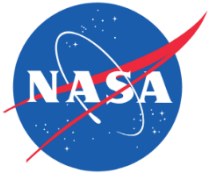


Model of System



Description of Tank System

- **Tank divided into Gas & Liquid Sides:**
 - Each side has 7 heaters, wired in parallel (14 heaters total)
 - Each circuit protected by an over-temperature TSTAT
- **Tank filled with Ar + GN2 gas mixture for TVAC test**
 - No propellant or simulant in tank during testing for safety and integration concerns
- **Temperature measured by non-flight sensors**
 - Digital 1-wire sensors, located throughout spacecraft
 - Some at same locations as flight thermistors
 - Flight thermistors limited in number and location



Thermal Vacuum Test Overview

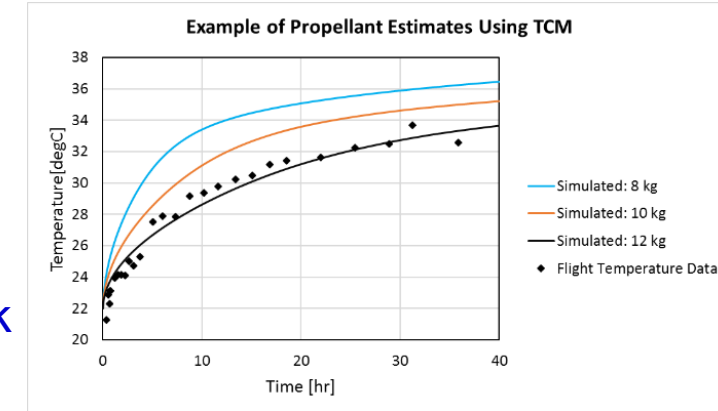
- **Thermal vacuum (TVAC) testing seeks to test entire spacecraft in a space-like environment**
 - Allows for test verification & correlation of thermal models
 - All subsystems perform tests to verify operation of components/equipment
- **Tank heater circuit over-temperature thermostat (TSTAT) test**
 - Verify operation of the two thermostats that control heater circuits on tank
 - Duplicates conditions of thermal capacitance gauging operation on orbit
 - Heats tank until over-temperature TSTAT set-point of 43°C is reached
 - Duration of test is approximately 6900s
- **Thermal model correlated with data from over-temp TSTAT test**
 - Heater current & temperature data from test fed into model
 - Model output compared to temperature data recorded by 1-wire sensors on tank



TCM Theory

- **Concept:**

- Heat is applied to tank and propellant via heaters
- Heat is conducted away by the structure and lost through radiation
- Monitor the temperature of the tank
- Temperature of the tank a function of the amount of propellant within the tank



Where:

\dot{Q} = rate of energy input (power)

c = specific heat

m = mass

$\frac{\partial T}{\partial t}$ = change in temperature WRT time

k = thermal conductivity

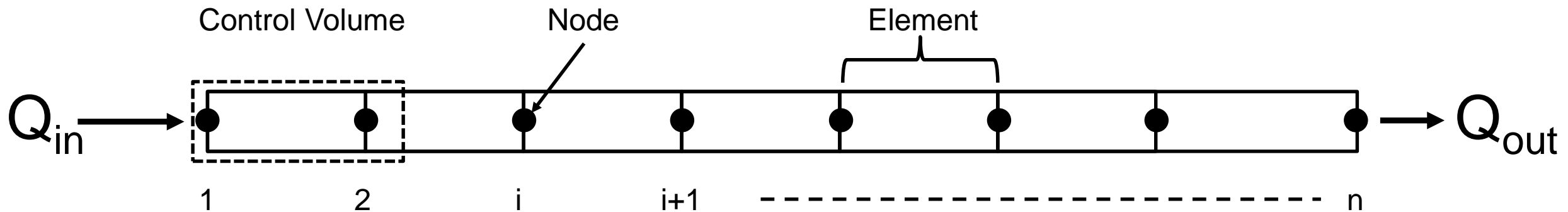
$$cm \frac{\partial T}{\partial t} = \dot{Q}_{in} - \dot{Q}_{loss} \quad (1)$$

$$\dot{Q}_{in} = \dot{Q}_{heaters} \quad (2)$$

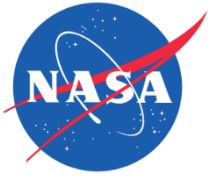
$$\dot{Q}_{loss} = \dot{Q}_{cond} + \dot{Q}_{rad} \quad (3)$$

TCM Theory (cont.)

- Energy conservation equation is solved using ANSYS Finite Element Analysis software
- Applies mesh to CAD solid model of system, creating finite elements
- Solver discretizes energy conservation equation at each node
- Equations form a linear system that is solved at each node at each time step in the model



1-D Rod Showing Elements, Nodes, & Control Volume



Main Assumptions

- **Convection within Gas in tank is neglected**
 - Mass of tank drives time constant of system, not mass of gas
 - Account for the mass of the gas
- **Radiation to environment modeled; surface-to-surface radiation neglected**
 - Surfaces temperatures within same magnitude (20-43°C)
 - Tank designed to minimize surface-to-surface radiation (low ϵ coatings & MLI blankets)
 - Radiation losses are negligible compared to conduction losses
- **Perfect bonded contact between interfaces**
 - Done to practically implement model within ANSYS
 - Correlation process will focus on changing the conductive resistances at interfaces to match test data

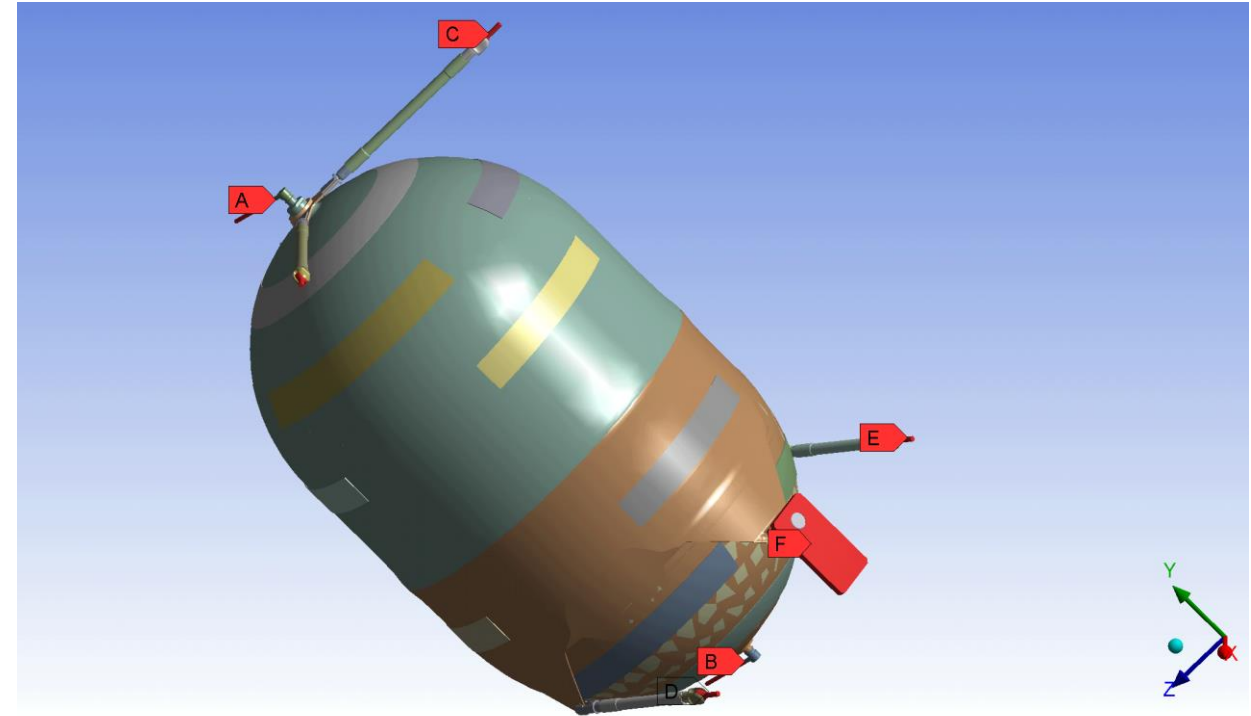
Initial & Boundary Conditions

- **Initial Conditions**

- Based upon 1-wire sensor readings
- Average temperature of 31°C used if no 1-wire was on or near a component

- **Boundary Condition: Temperature**

- Tank interface temperatures were monitored during by 1-wire sensors
- Allowed model to be simplified by removing support structure



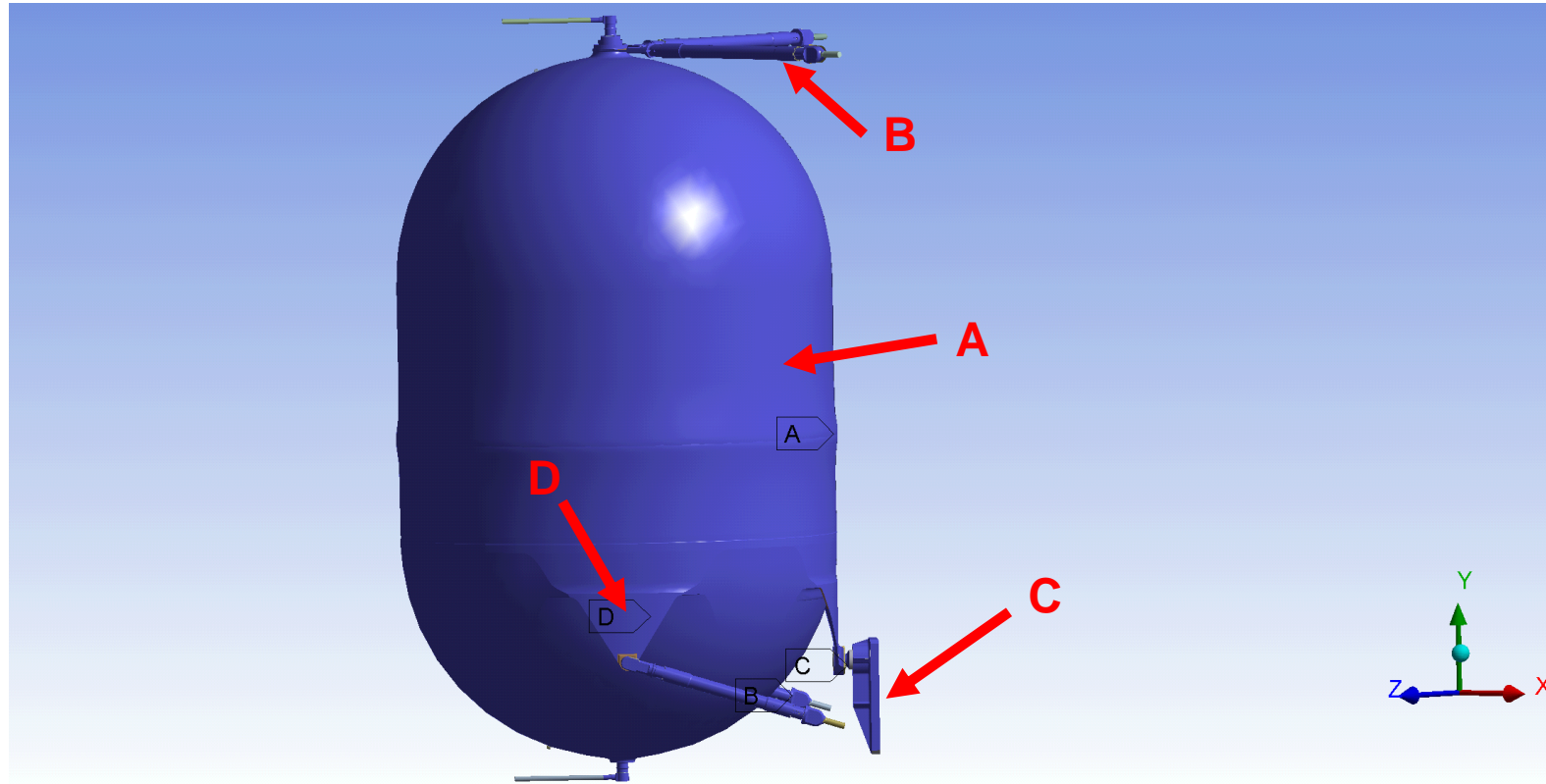
Location of Temperature Boundary Conditions

Boundary Conditions: Radiation

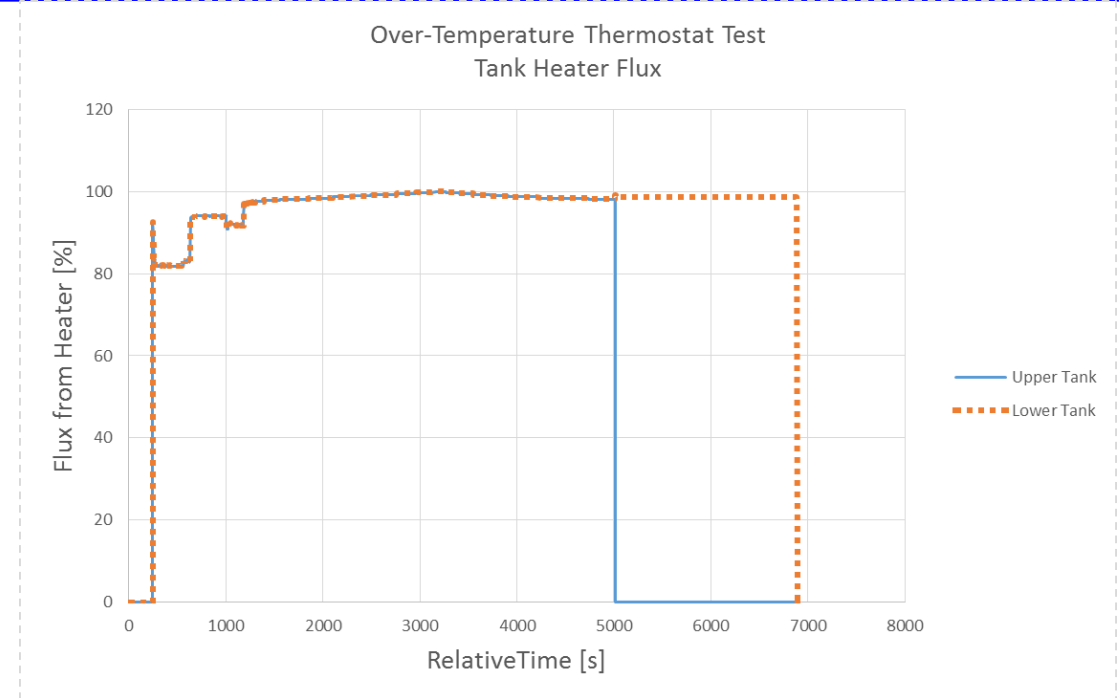
- Radiation transfer to environment modeled
- Applied emissivities of tank blankets and parts

Optical Properties	Emissivity	Ambient Temp (°C)
Axial Pin & Receiver	0.85	31
Exposed Tank Tabs	0.15	33
Struts	0.15	31
Tank Blanket	4.50E-03	31

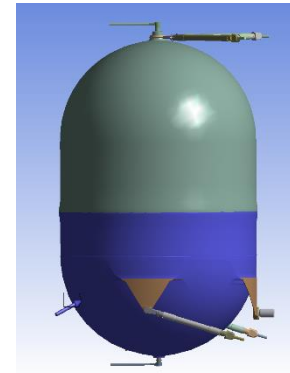
Label	Definition
A	Blanket
B	Struts
C	Tank Pin & Receiver Plate
D	Tank Exposed Parts (tabs, etc.)



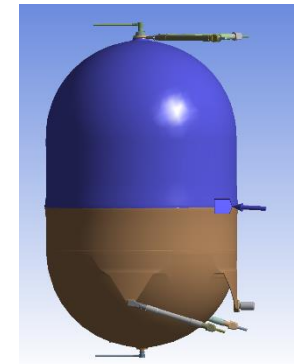
- Heat input provided by the tank heaters
- Uniformly distributed heat flux over upper & lower tank surfaces
 - Tank and heaters covered aluminum tape with conductive adhesive
 - Meant to evenly spread heat around tank
- Heater power and on-times determined using heater circuit current data



Lower Hemisphere

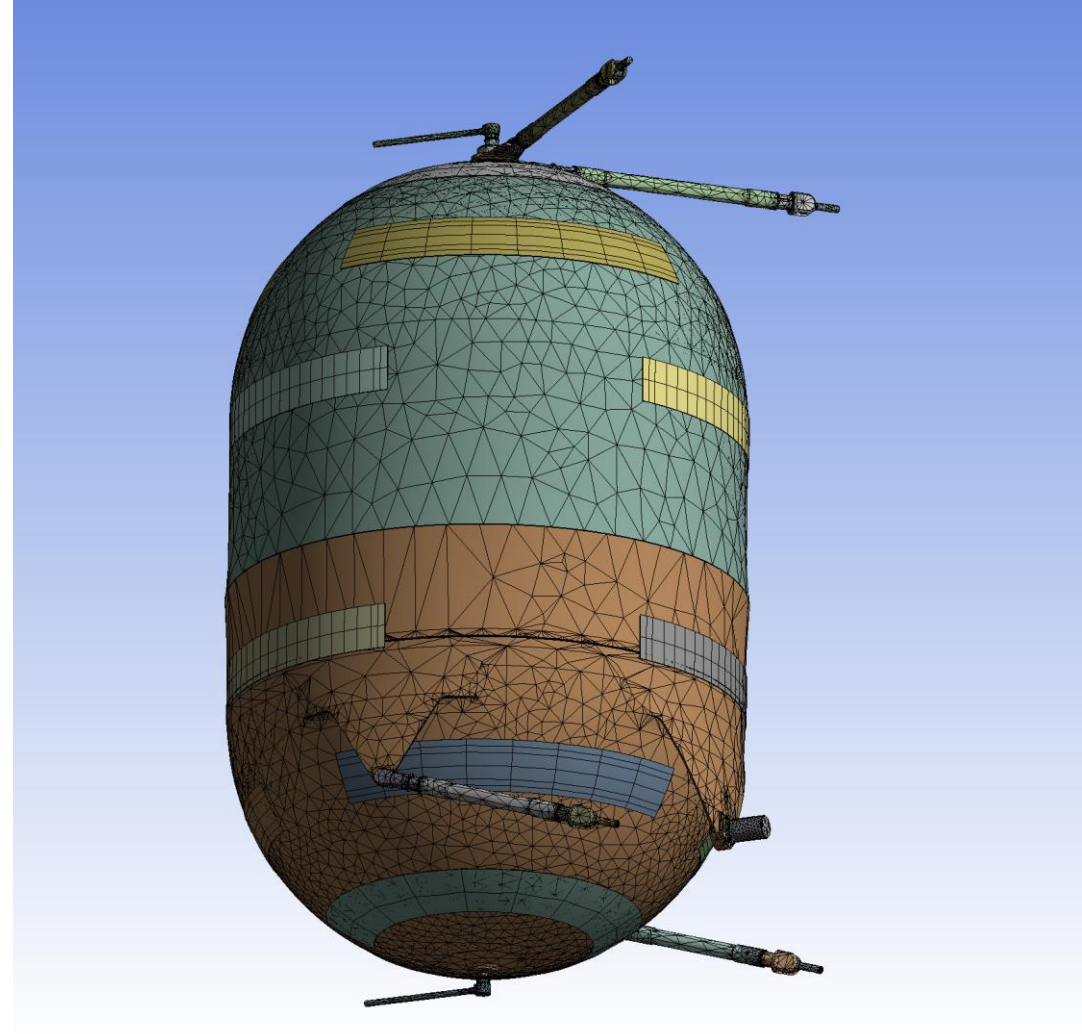


Upper Hemisphere



Mesh

- Created with ANSYS automatic mesh controls
- Generated patch-conforming/sweeping mesh
 - ~175,000 nodes and 88,400 elements

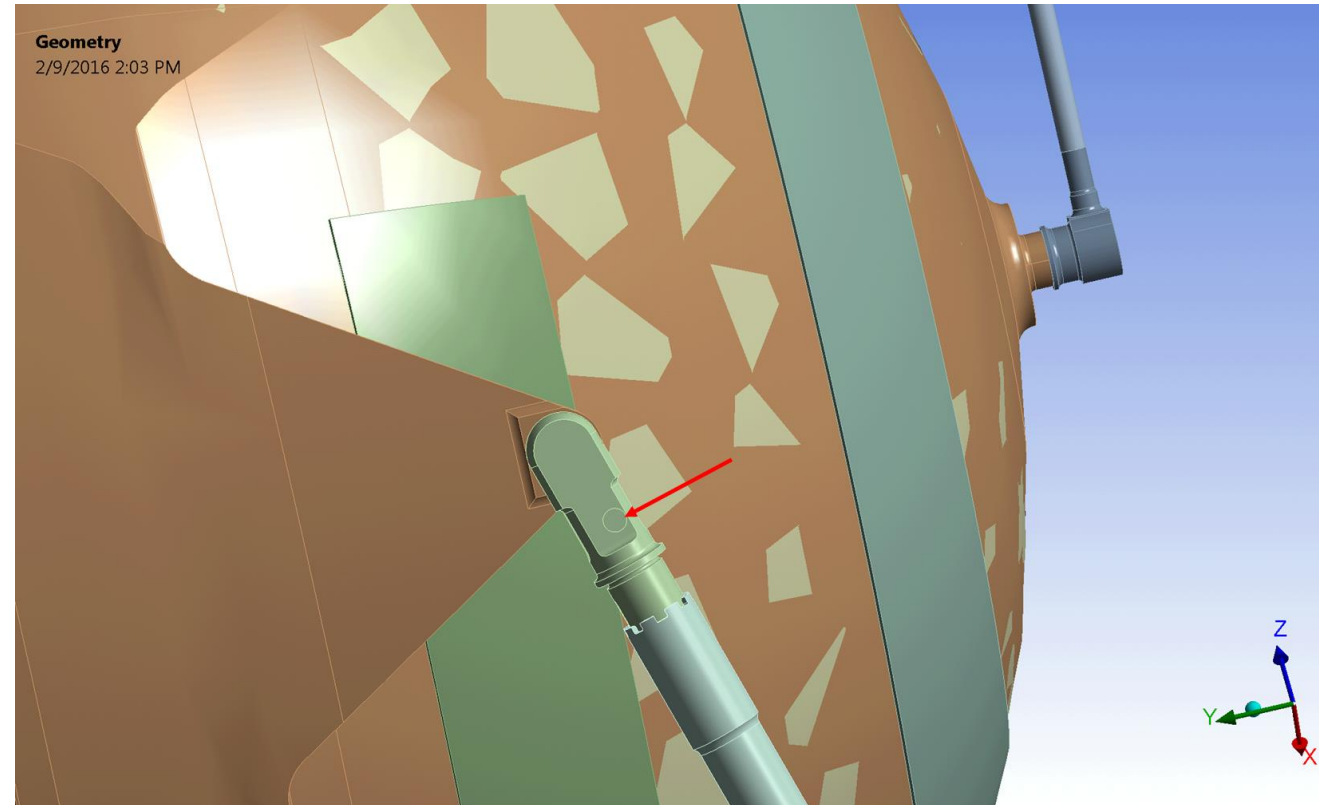


Sensor Locations

- Defined locations on tank model that matched as-bonded location of 1-wire sensors

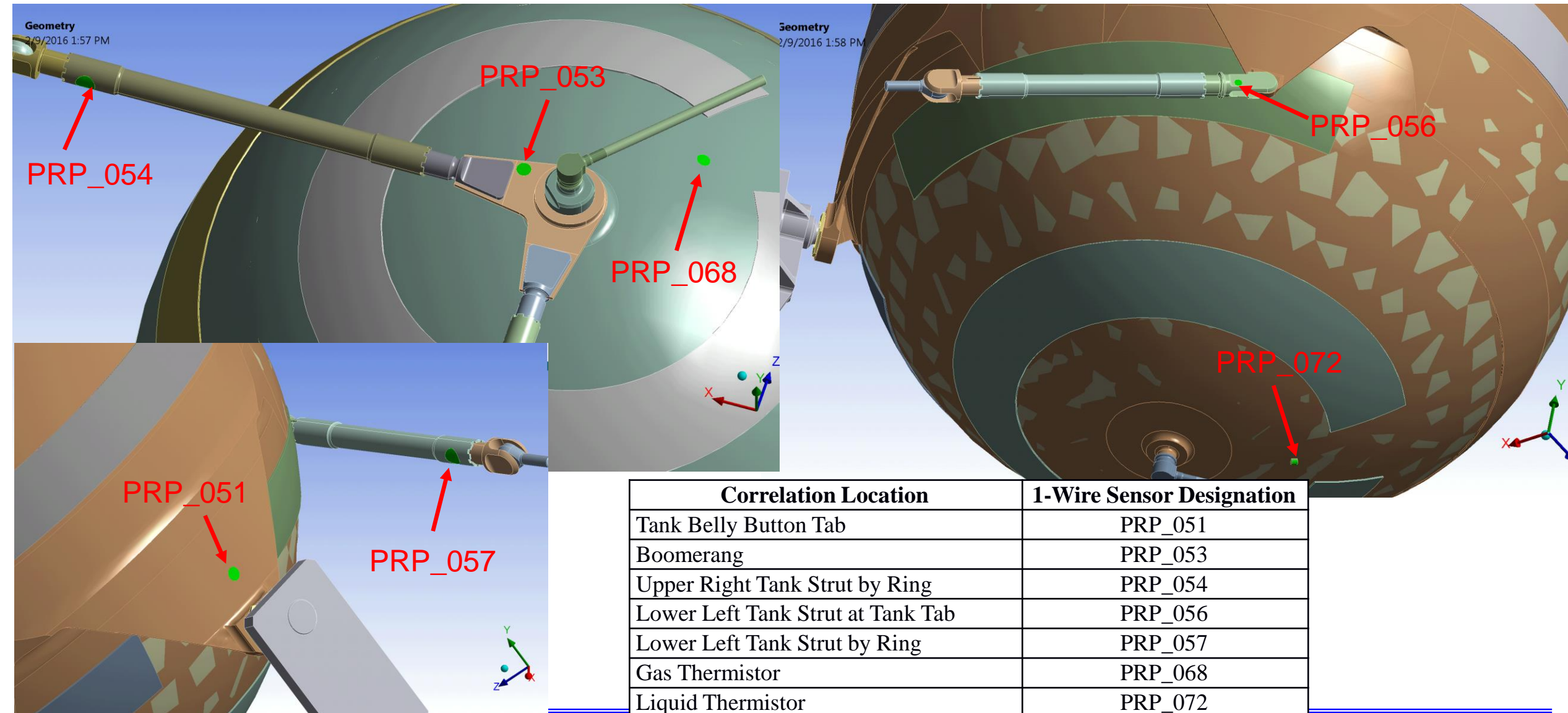


Flight Location




Model Location

Sensor Locations (cont.)



Correlation Location	1-Wire Sensor Designation
Tank Belly Button Tab	PRP_051
Boomerang	PRP_053
Upper Right Tank Strut by Ring	PRP_054
Lower Left Tank Strut at Tank Tab	PRP_056
Lower Left Tank Strut by Ring	PRP_057
Gas Thermistor	PRP_068
Liquid Thermistor	PRP_072

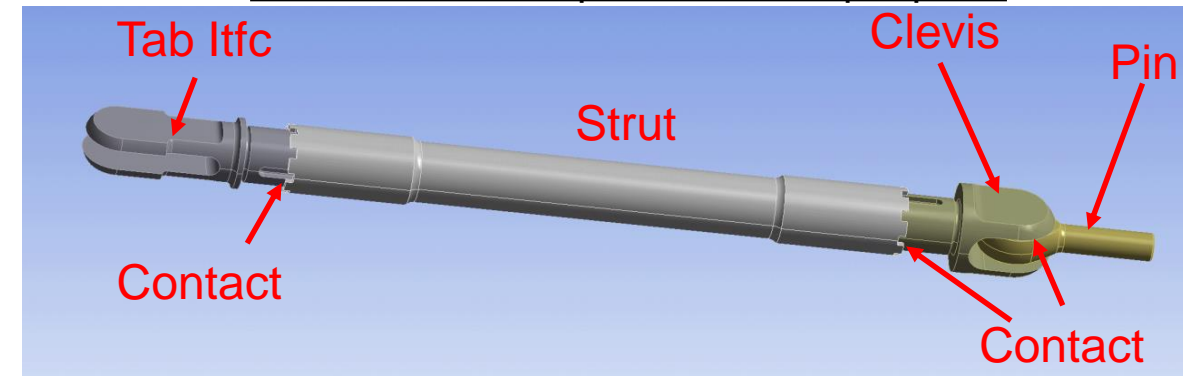
Correlation Process

- **Translate: real tank**  **model of tank**
 - Model approximation of reality
 - Account for approximation by adjusting thermal resistances in model to match test data
- **Thermal Conductance, U : adjust thermal resistance**

$$Q = -U\Delta T \quad (8)$$

$$U = \frac{kA}{L} \quad (9)$$

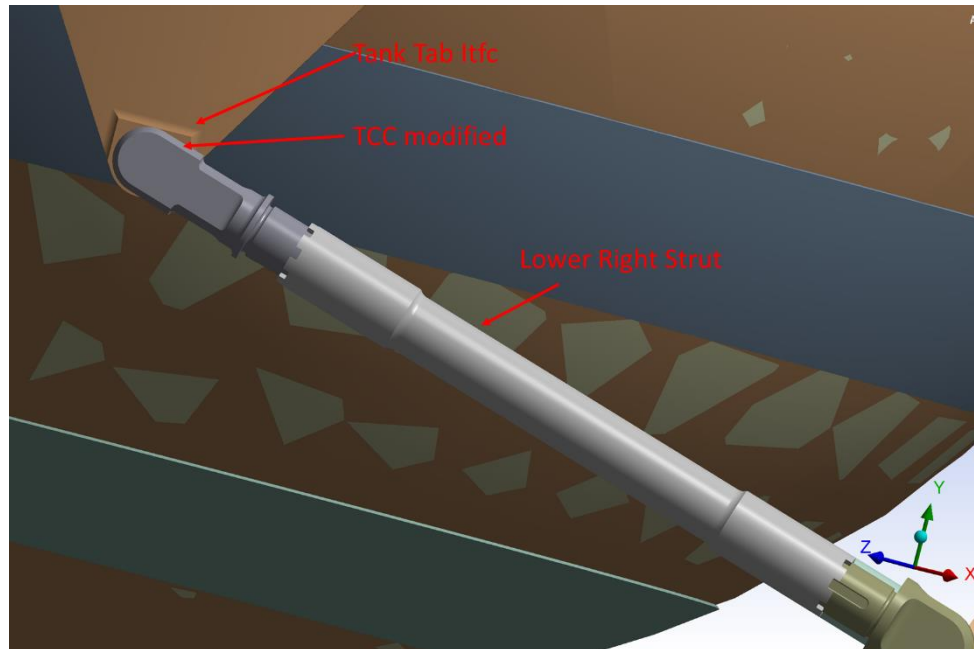
Tank Strut is composed of multiple parts



- **Match test data by modifying thermal contact conductance (TCC) of tank parts**
- **Limitation with ANSYS:**
 - Modify TCC at contact regions only, but not for group of parts
 - Modified conductance by using a conductivity multiplier

Conductance Studies: Study #1

- 1) Lower Tank Strut at Tab Interface
- Goal: match temperatures at Lower Left Strut Tab and Liquid Sensor
 - Altered TCC at strut tabs
 - Altered lower hemisphere conductivity multiplier to account for tape on tank
 - Increased strut overall conductivity multiplier to account for electrical harness

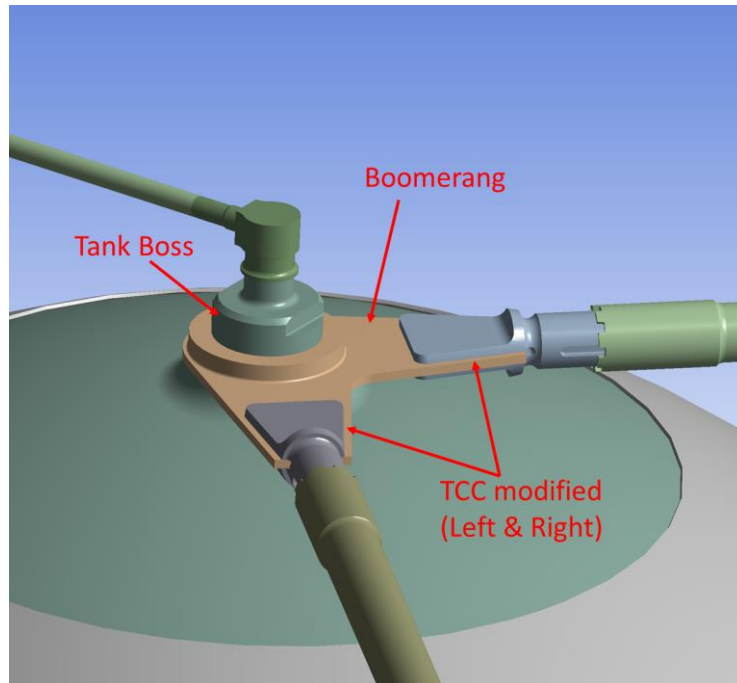


Rev	Lower Strut TCC at Tank Tabs			Difference of Model - Measured Temp (°C)		
	Right TCC	Left TCC	Lower Hemi k	Liq (PRP_072)	Belly Button Tab (PRP_051)	LL Strut Tab (PRP_056)
31	20	20	1.5x	3.415	3.723	1.08
29	50	50	1.5x	3.402	3.714	3.563
28	75	75	1.5x	3.397	3.711	4.363
27	127	127	1.5x	3.391	3.707	5.112
30	175	175	1.5x	3.389	3.706	5.43
32	20	20	2.0x	2.538	3.815	1.392
33	20	20	2.0x	2.439	0.473 ^a	1.293

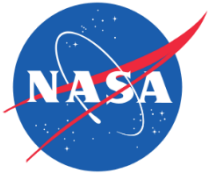
^a In this Rev, results were queried from a patch area instead of a full selected area

Conductance Studies: Study #2

- 2) Boomerang
- Goal: Increase heat flux into upper hemisphere and match temperatures at Boomerang
 - Altered TCC
 - Altered upper hemisphere conductivity multiplier to account for effect of tape on tank

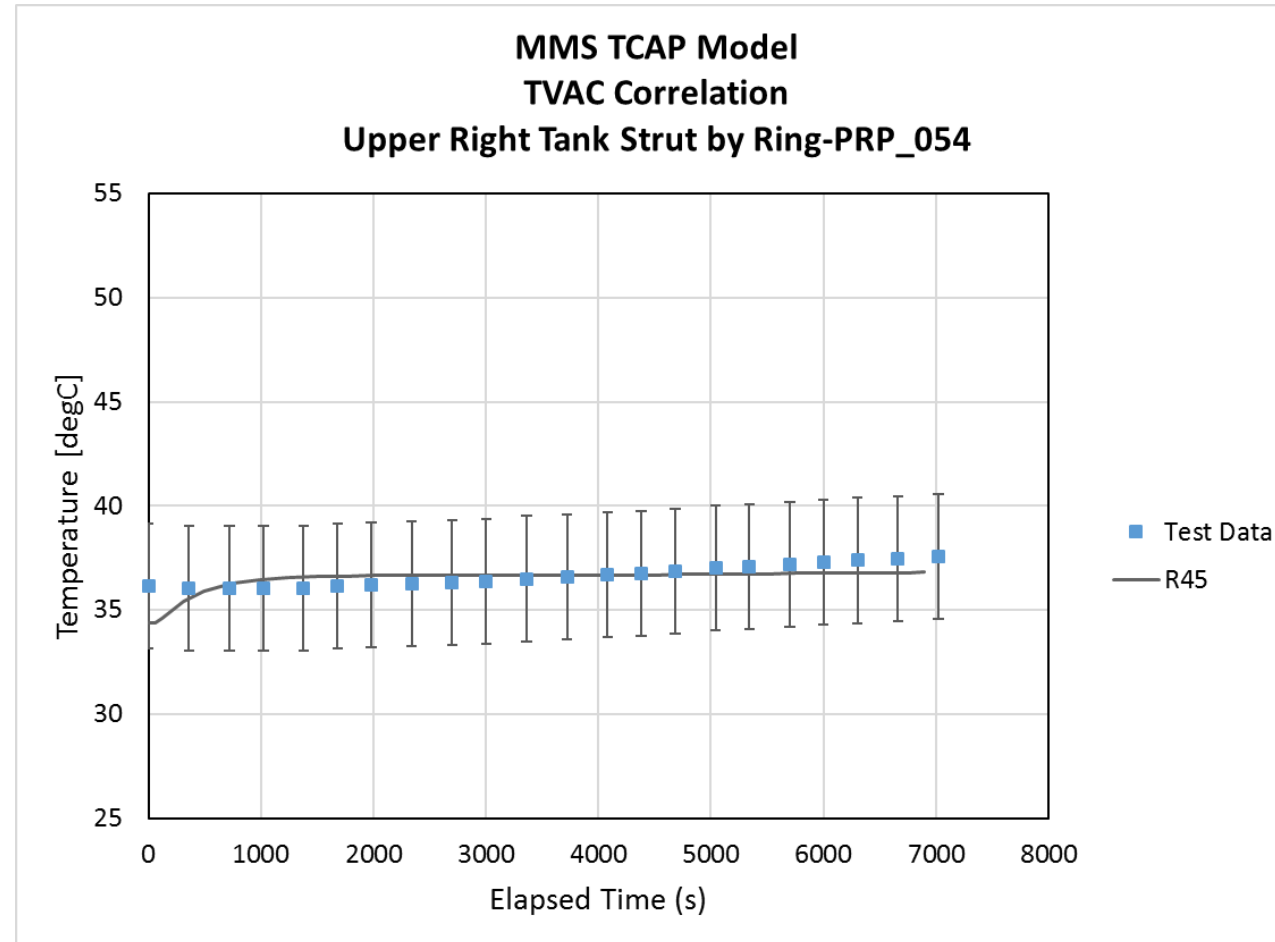


Rev	Boomerang		Upper Hemi k	Difference of Model - Measured Temp (°C)				
	Right TCC	Left TCC		Liq (PRP_072)	Belly Button Tab (PRP_051)	Upper Strut (PRP_054)	LL Strut Tab (PRP_056)	Boomerang (PRP_053)
39	150	150	1.0x	2.47	0.471	-0.743	1.298	-2.048
40	100	100	1.0x	2.47	0.471	-0.747	1.298	-1.997
41	20	20	1.0x	2.47	0.471	-0.773	1.298	-1.584
45	20	20	1.5x	2.545	0.575	-0.756	1.365	-1.049



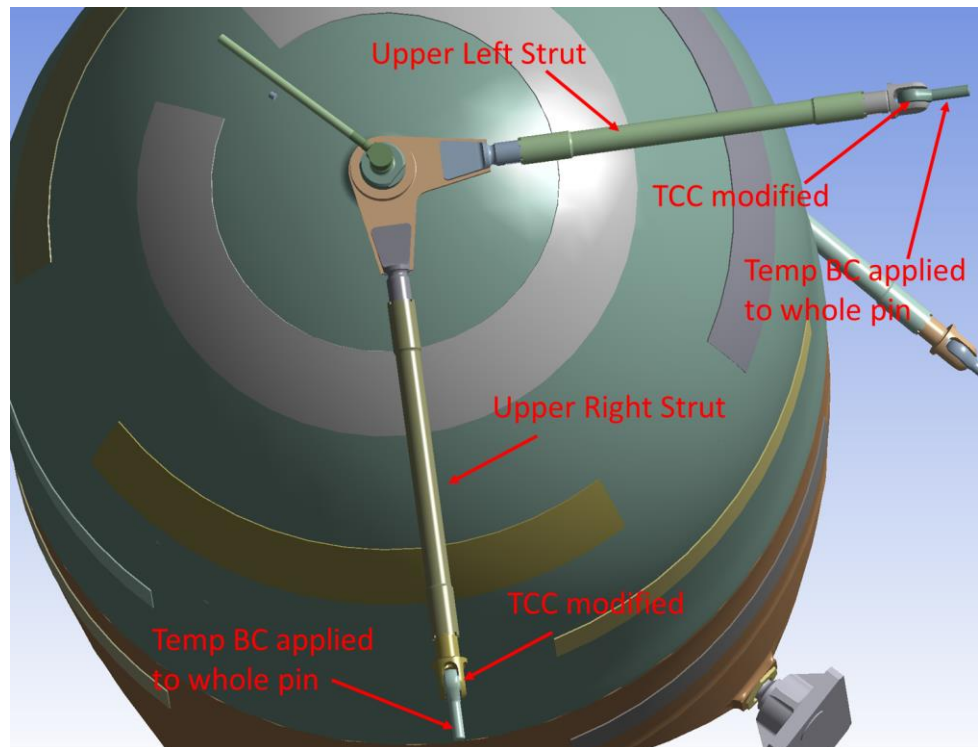
Conductance Studies: Study #2

- 2) Boomerang (cont.)
- Found that physics were not matched at Upper Strut



Conductance Studies: Study #3

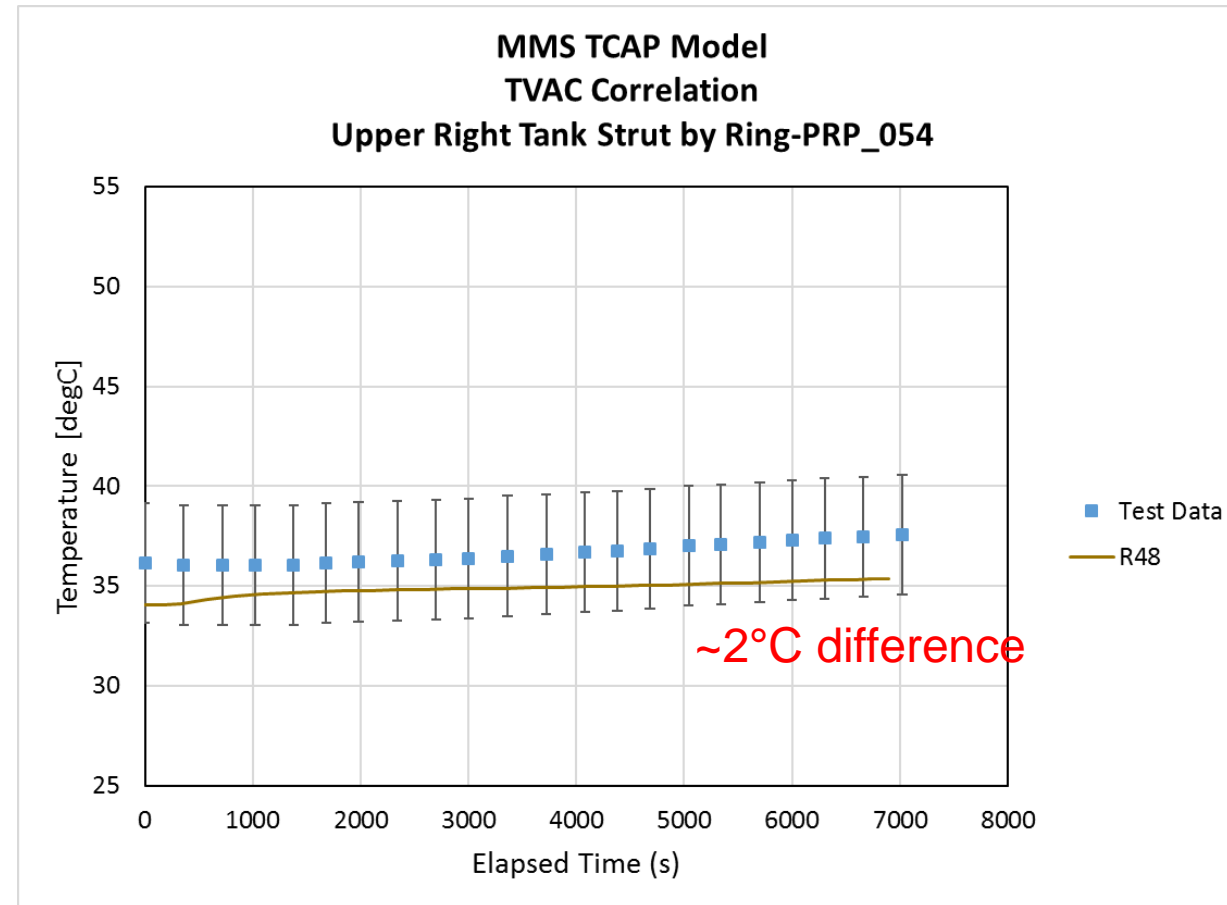
- 3) Upper Strut End Conductance Study
- Goal: Match physics at Upper Struts
 - Reduced TCC on pins caused temperature difference was getting larger
 - Increased TCC on pins & adjusted strut conductivity multipliers: marked improvement in physics



Rev	Upper Strut TCC at Pin				Difference of Model - Measured Temp (°C)			
	Right TCC	Left TCC	Upper Right Strut k	Upper Hemi k	Liq (PRP_072)	Upper Strut (PRP_054)	LL Strut Tab (PRP_056)	Boomerang (PRP_053)
42	150	150	1.5x	1.0x	2.374	-2.482	1.315	-2.389
43	100	100	1.5x	1.0x	2.374	-2.951	1.315	-2.401
44	50	50	1.5x	1.0x	2.373	-3.757	1.315	-2.418
46	50	50	2.5x	1.5x	2.447	-3.468	1.302	-2.366
47	100	100	2.5x	1.5x	2.447	-2.686	1.302	-2.33
48	150	150	2.5x	1.5x	2.447	-2.212	1.302	-2.307

Conductance Studies: Study #3

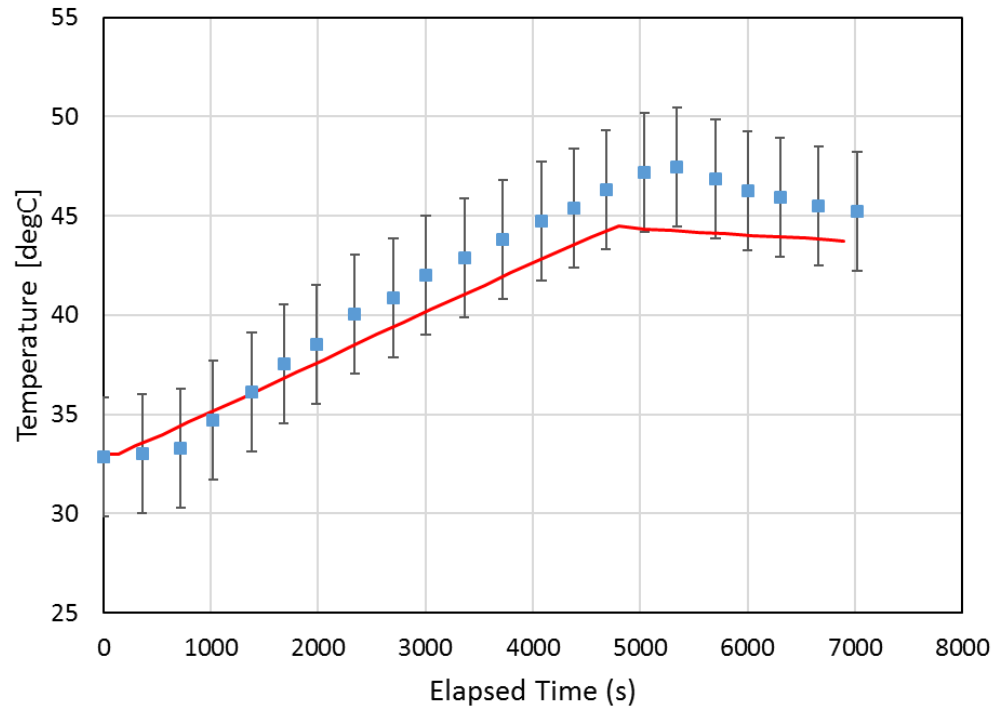
- 3) Upper Strut End Conductance Study (cont.)
 - Able to improve trend in modeled temperature response, particularly after ~1000s of sim. time
 - Larger temperature difference than previously, but better match test data overall



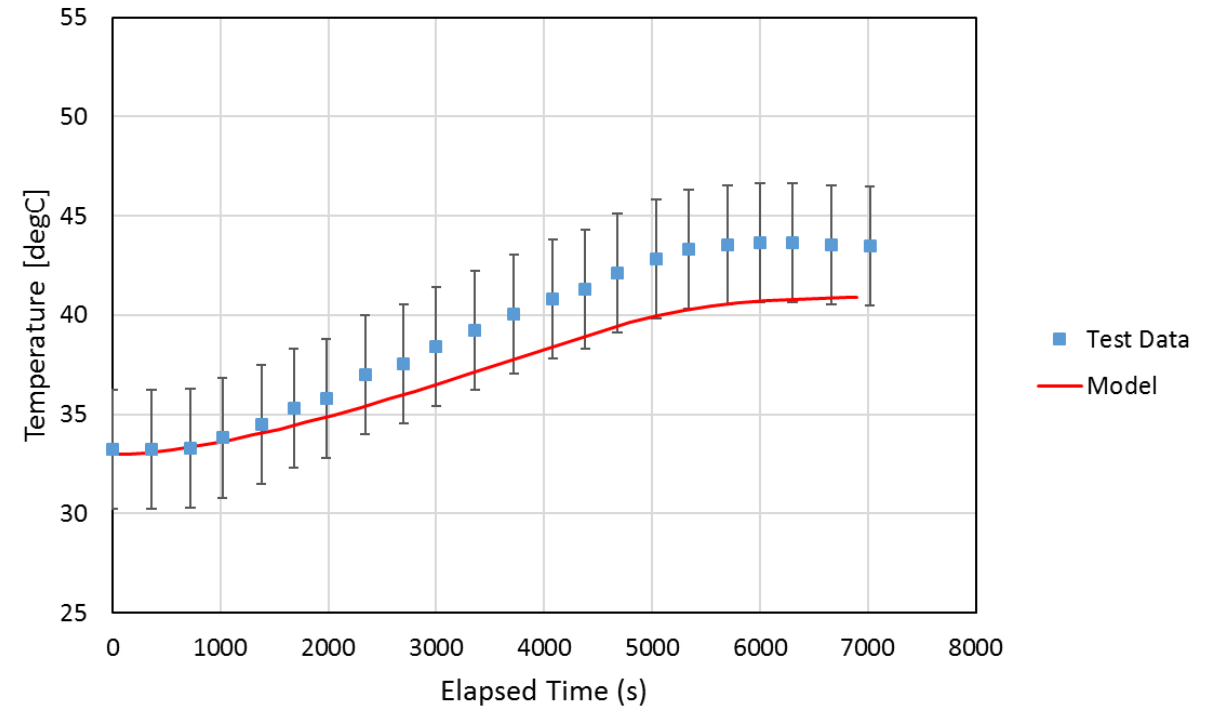


Results: Gas (Top) Side

MMS TCAP Model
TVAC Correlation
Gas Thermistor-PRP_068

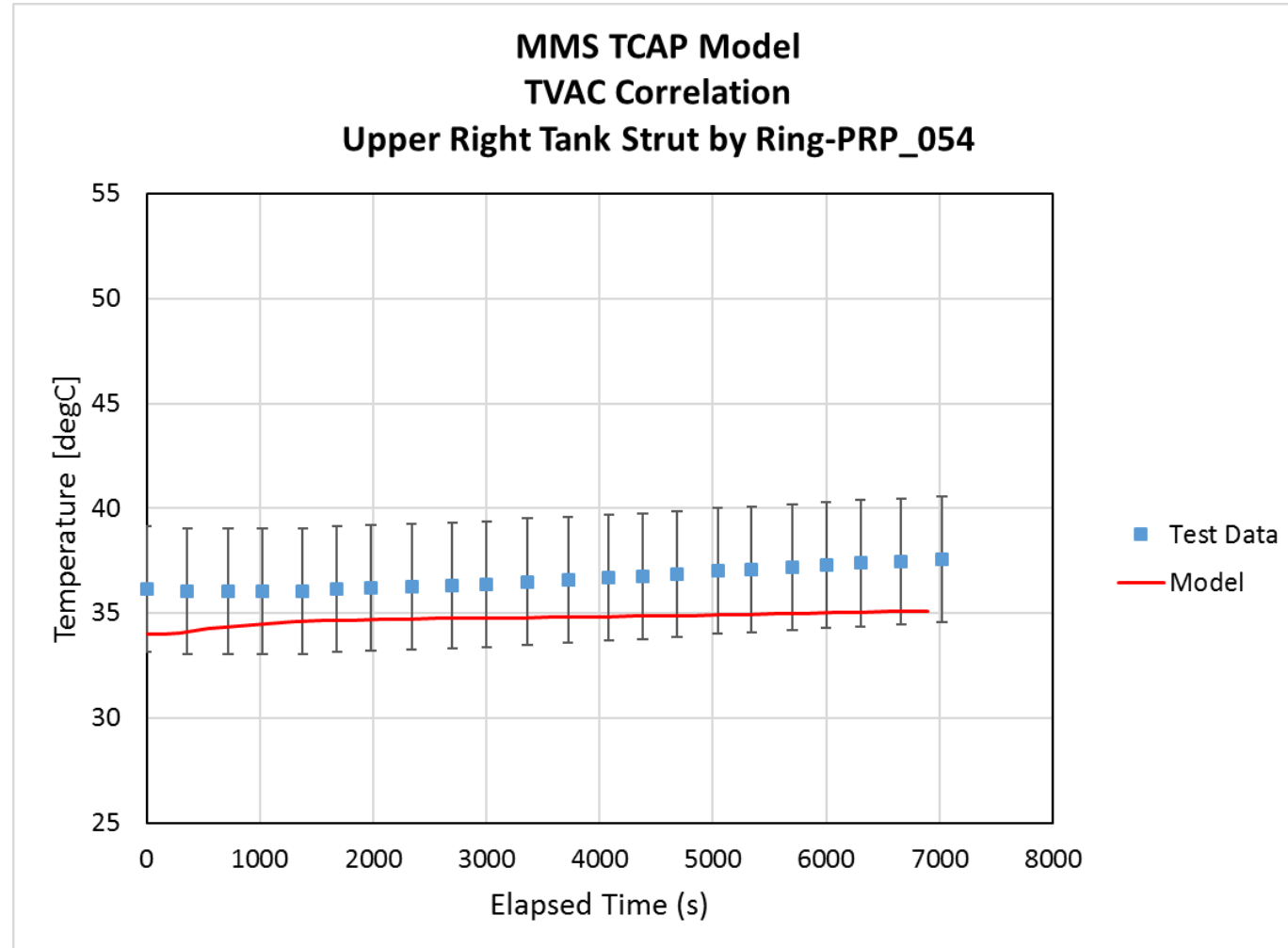


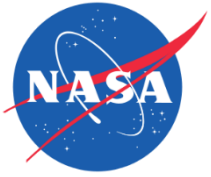
MMS TCAP Model
TVAC Correlation
Boomerang-PRP_053





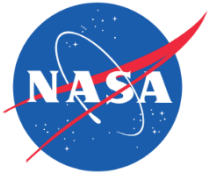
Results: Gas (Top) Side





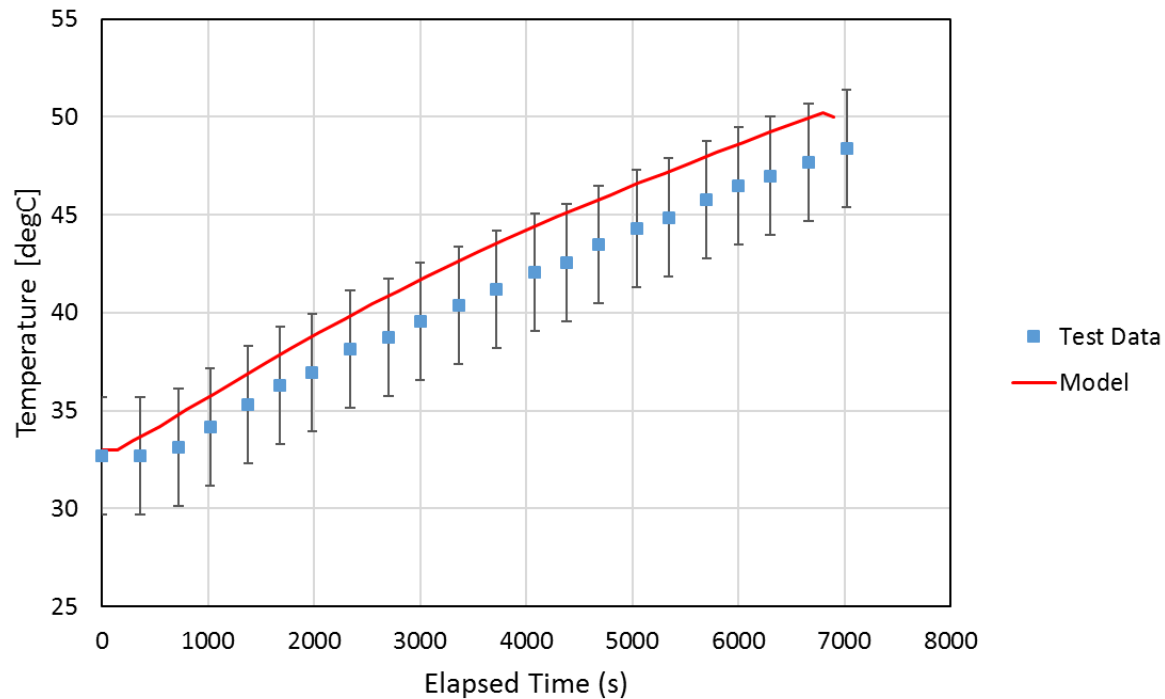
Discussion: Gas (Top) Side

- **Model output within $\pm 3^{\circ}\text{C}$ for all sensors**
- **Under predicted temperatures at all sensor locations**
- **Trends in temperature rise in time match trends in test data**
 - Main physics are being captured
- **Analyzed results at Gas Thermistor Location (PRP_068)**
 - Approached -3°C limit at 5000-6000s
 - Peak temperature: 2.7°C lower & $\sim 900\text{s}$ earlier
 - Slope of simulated temperature: $\sim 0.15^{\circ}\text{C}/\text{min}$ (Test data: $\sim 0.19^{\circ}\text{C}/\text{min}$)
- **Boomerang Location (PRP_053) show similar trends to Gas Location**
- **Likely Cause:**
 - Uniformly applied heat flux removes higher localized heat flux \rightarrow lower temperatures
 - Further investigation of this is subject of future work

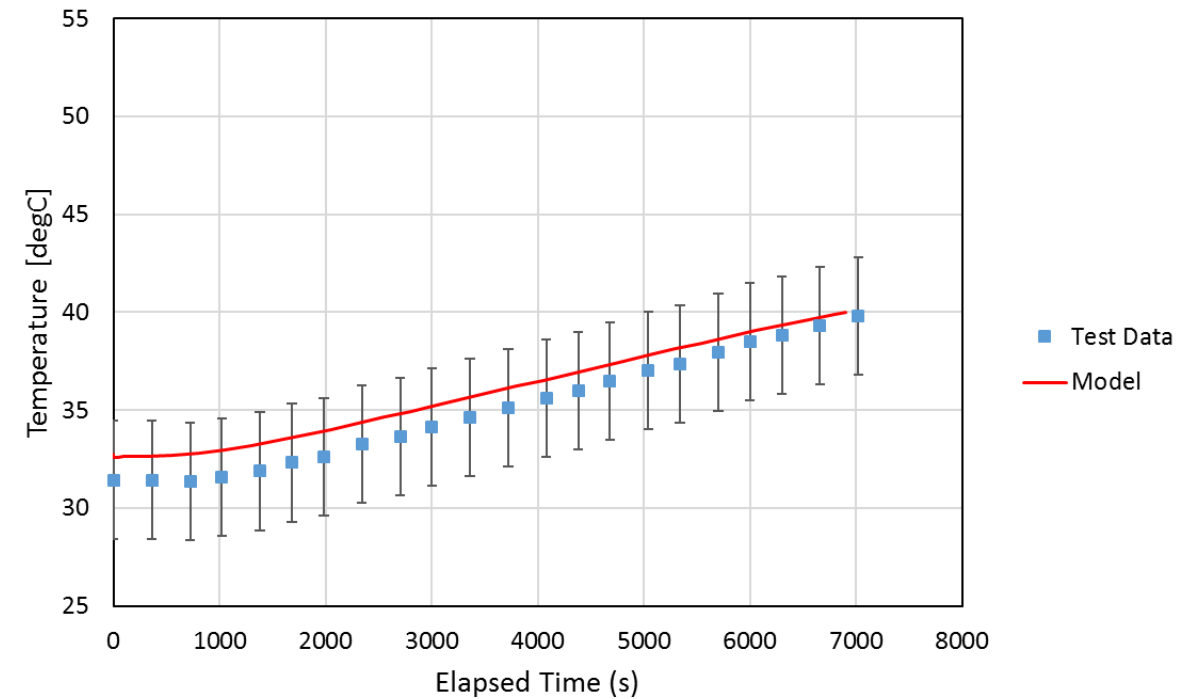


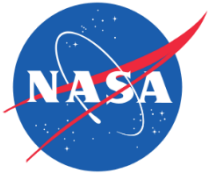
Results: Liquid (Bottom) Side

MMS TCAP Model
TVAC Correlation
Liquid Thermistor-PRP-072



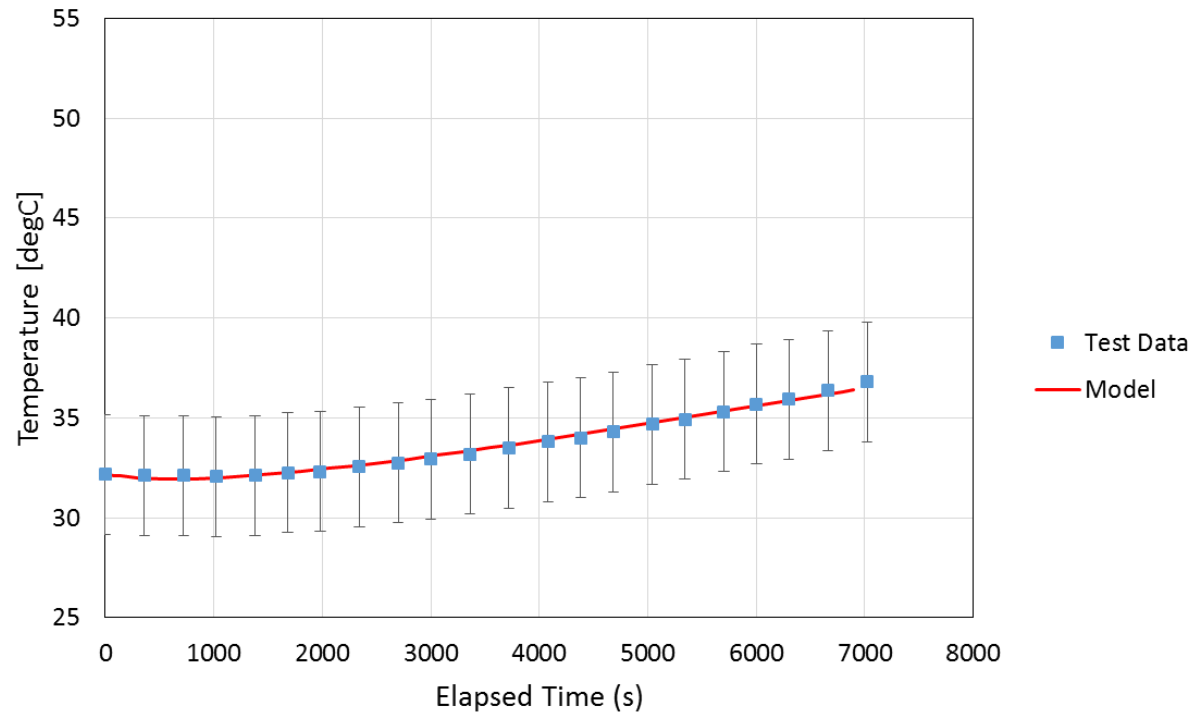
MMS TCAP Model
TVAC Correlation
Tank Belly Button Tab-PRP_051



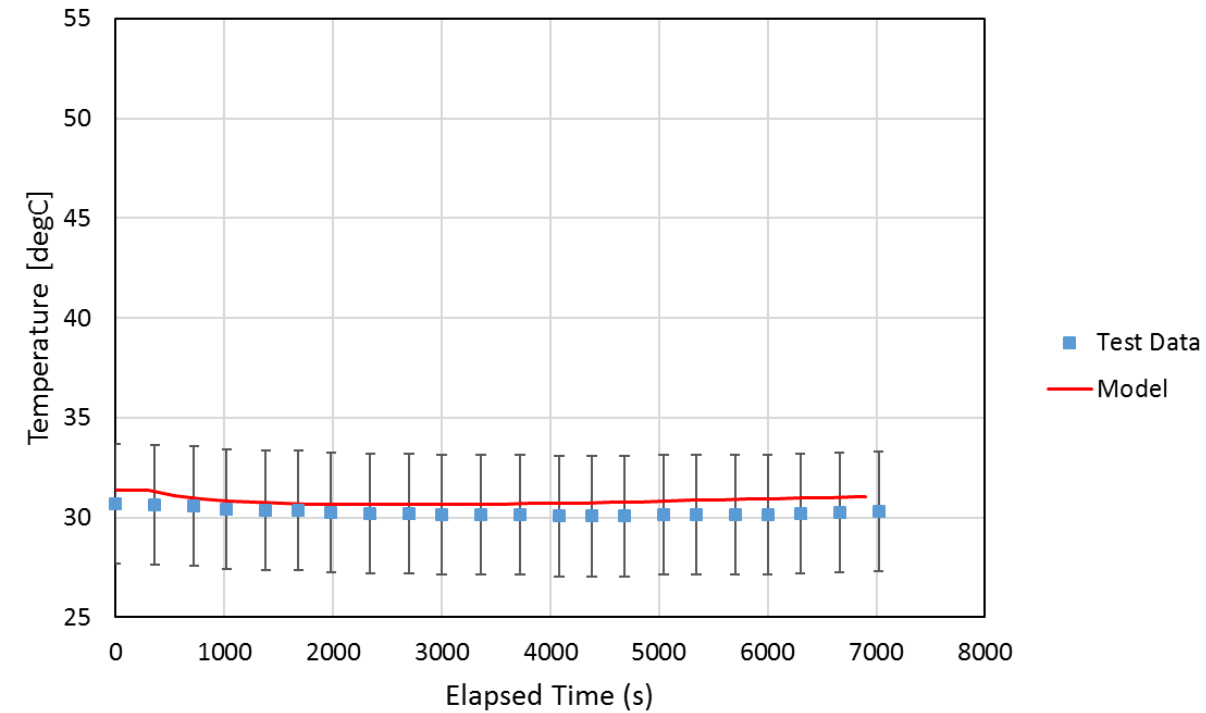


Results: Liquid (Bottom) Side

MMS TCAP Model
TVAC Correlation
Lower Left Tank Strut at Tank Tab-PRP_056



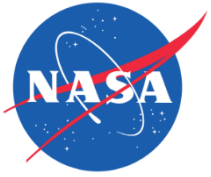
MMS TCAP Model
TVAC Correlation
Lower Left Tank Strut by Ring-PRP_057





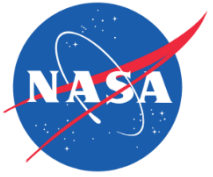
Discussion: Liquid (Bottom) Side

- **Model output within $\pm 3^{\circ}\text{C}$ for all sensors**
- **Trends in temperature rise in time match trends in test data**
 - Main physics are being captured
- **Model over-predict results at half of the sensor locations**
 - Exceptions: PRP_056 and PRP_057, showed good agreement with test data
- **Slopes better matched test data:**
 - PRP_072: $0.16^{\circ}\text{C}/\text{min}$ (Test data: $0.15^{\circ}\text{C}/\text{min}$)
- **Over-predictions likely due to larger heat flux in bottom half of model**
 - Consistent with gas side, where opposite affect was observed
 - Further investigation of this is subject of future work

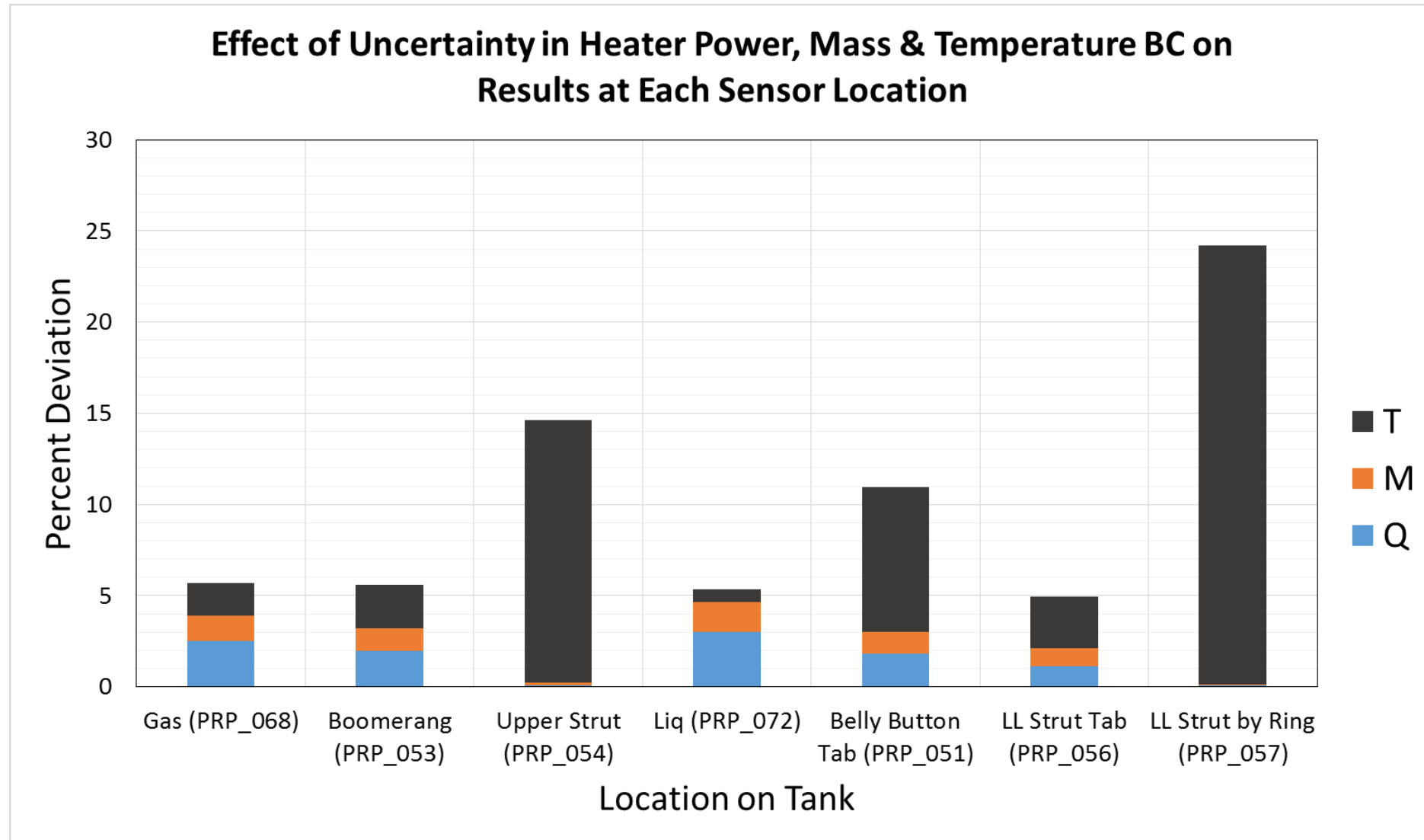


Uncertainty Analysis

- **Conducted to understand impacts on predicted temperature results**
- **Heat Flux:**
 - 9.6% uncertainty due to worst-case heater & current measurement error
- **Mass of Tank:**
 - Crane scale measurement (1.13 kg worst case error)
- **Temperature Boundary Conditions:**
 - Lack of flight sensors at each strut to ring interface
 - Bounded worst-case range of +/- 10°C

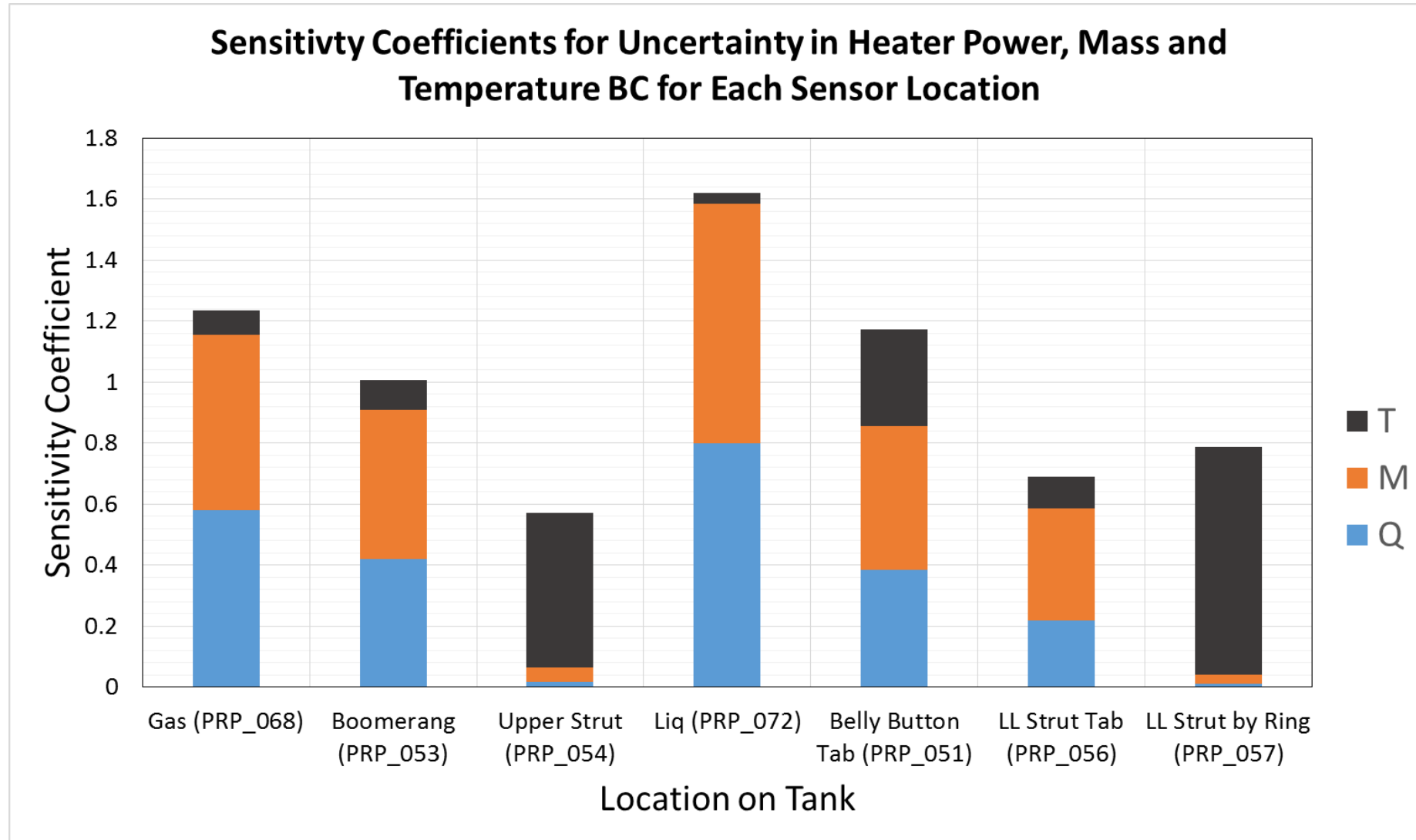


Uncertainty Analysis Results





Uncertainty Analysis Results (cont.)





Uncertainty Analysis Discussion

- **Percent Deviation:**

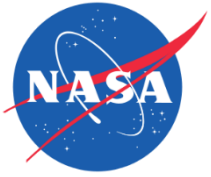
- Uncertainty in applied heater power has largest effect
- Temperature BC uncertainty has largest effect only near tank interface locations

- **Sensitivity:**

- Model is sensitive to uncertainties in applied heater power & Mass
- ~10% change in heater power results in 1-2°C difference in predicted temperatures at tank poles
- 0.9°C per 1 kg of mass uncertainty

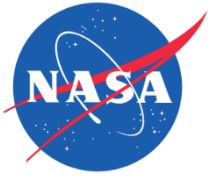
- **Conclusions:**

- Uncertainties in heat flux lead to higher percent deviations in the model, with uncertainties in temperature BC only affecting predictions of interface temperatures
- Model most sensitive to uncertainties in heat flux and mass



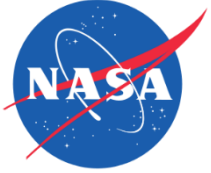
Conclusions

- **The project objective has been met:**
 - The thermal model developed was able to predict temperatures within the acceptance criterion of $\pm 3^{\circ}\text{C}$.
 - It is therefore sufficient to make future propellant estimates for the MMS spacecraft
- **Model found to be sensitive to uncertainties in applied heater power and total tank mass**
- **The cause of the discrepancy in under-predicted temperatures on the gas side of tank and over-predicted temperatures on the liquid side of the tank needs to be investigated further and addressed in future work**



Issues

- **Over-complexity of ANSYS model**
 - Details of CAD model of MMS tank system can only be reduced so much within ANSYS
 - Grouping of parts to address issues with modeling contact and thermal conductance was cumbersome
- **Simulation Solve Time**
 - High level of detail resulted in dense mesh; this increased solve time significantly
 - Solve times: 45 min per run (over 65 runs were completed, or over 48 hours of continuous solve time)
 - Comparison: entire MMS spacecraft thermal model (made in Thermal Desktop) took 20 minutes to solve



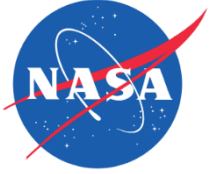
Key Lesson Learned

- **Model is an approximation of reality**
 - Have to make assumptions to practically implement model and account for behavior of real model
- **Add complexity incrementally, rather than remove complexity**
- **Understand how software queries results from model**



Future Work

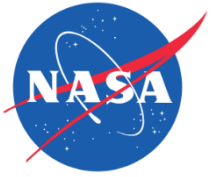
- **Address uniform heat flux BC to improve Gas-Side temperature results**
- **Address model complexity: Thermal Desktop implementation**
- **Add surrounding structure: Account for uncertainties in temperature boundary conditions**
- **Start Phase III of project: flight calibration and propellant estimations**



Acknowledgements

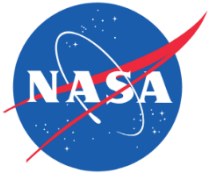
I would like to thank and acknowledge the following individuals who provided invaluable time, experience and guidance such that this project could be completed.

- Dr. Christopher Cadou, Department of Aerospace Engineering, University of Maryland (Advisor)
- Dr. Eric Cardiff, Code 597 Propulsion Branch, Goddard Space Flight Center (NASA Advisor)
- Dr. Raymond Sedwick, Department of Aerospace Engineering, University of Maryland (Committee Member)
- Dr. Bao Yang, Department of Mechanical Engineering, University of Maryland (Committee Member)
- Sunil Acharya, Mallett Technologies
- Chris Anders, Code 540, Mechanical Systems Division
- Mike Commons, Code 545 Thermal Branch, Goddard Space Flight Center
- Eric Grob, Code 545 Thermal Branch, Goddard Space Flight Center
- Jong Kim, Code 545 Thermal Branch, Goddard Space Flight Center
- Joe Miller, Code 597 Propulsion Branch, Goddard Space Flight Center
- Mike Rife, Mallett Technologies
- Jason Solimani, Code 545 Thermal Branch, Goddard Space Flight Center
- Eric Stoneking, Code 591 Guidance, Navigation and Control Systems Branch, Goddard Space Flight Center
- Dewey Willis, Code 597 Propulsion Branch, Goddard Space Flight Center
- Kurt Wolko, Code 597 Propulsion Branch, Goddard Space Flight Center



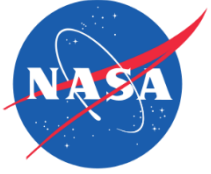
References

1. David G. Gilmore, editor. *Spacecraft Thermal Control Handbook, Vol. 1: Fundamental Technologies*, volume 1, chapter 19, page 724. The Aerospace Press, El Segundo, CA, second edition, 2002. Fig. 19.3.
2. National Aeronautics and Space Administration. Unlocking the Secrets of the Electron Diffusion Region. The Magnetospheric Multiscale (MMS) Mission, Mar 2016. Web. Accessed 05-Feb-2016. <http://mms.gsfc.nasa.gov/science.html>.
3. Boris Yendler and T. Narita. Thermal Propellant Gauging System for BSS 601. In 25th AIAA International Communications Satellite Systems Conference (organized by APSCC). International Communications Satellite Systems Conferences (ICSSC), AIAA, April 2007. doi:10.2514/6.2007-3149.
4. Boris Yendler. Unconventional Thermal Propellant Gauging System. In 45th AIAA Aerospace Sciences Meeting and Exhibit. Aerospace Sciences Meetings, AIAA, January 2007. doi:10.2514/6.2007-1363.
5. Andres Aparicio and Boris Yendler. Thermal Propellant Gauging at EOL, Telstar 11 Implementation. In SpaceOps 2008. SpaceOps Conferences, AIAA, May 2008. doi:10.2514/6.2008-3375.
6. Boris Yendler, Ibrahim Oz, and Lionel Pelenc. Thermal Propellant Gauging, SpaceBus 2000 (Turksat 1C) Implementation. In AIAA SPACE 2008 Conference & Exposition. SPACE Conferences and Exposition, AIAA, September 2008. doi:10.2514/6.2008-7697.

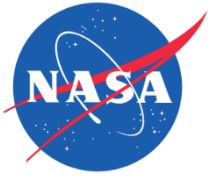


References (cont.)

7. Boris Yendler. Implementation of Thermal Gauging Method for SpaceBus 3000A (ArabSat 2B). In SpaceOps 2012 Conference. SpaceOps Conferences, AIAA, June 2012. doi:10.2514/6.2008-7697.
8. Boris Yendler and S. Chernikov. Comparison of Gauging Methods for Orbital's GEOStar 1 Satellites. In SpaceOps 2014 Conference. SpaceOps Conferences, AIAA, May 2014. doi:10.2514/6.2014-1810.
9. Boris Yendler, S. Chernikov, et al. Implementation of Thermal Gauging Method for Orbital Sciences Corporation's GEOStar 1 Satellite. In SPACE 2013 Conference and Exposition. SPACE Conferences and Exposition, AIAA, September 2013.
10. National Aeronautics and Space Administration. Magnetospheric Multiscale Observatory Integration. The Magnetospheric Multiscale (MMS) Mission, March 2016. Web. Accessed 10-Feb-2016. http://mms.gsfc.nasa.gov/observatory_integration/obs1/obs1_07.html.
11. Joseph Miller, Stephen McKim, et al. TRMM Remaining Fuel Estimation Report. Internal NASA Presentation, Goddard Space Flight Center, Code 597, August 2013.
12. M. V. CHOBOTOV and G. P. PUROHIT. Low-gravity propellant gauging system for accurate predictions of spacecraft end-of-life. *Journal of Spacecraft and Rockets*, 30(1):92–101, January 1993. doi: 10.2514/3.25475.
13. Amit Lal and B.N. Raghunandan. Uncertainty analysis of propellant gauging system for spacecraft. *Journal of Spacecraft and Rockets*, 42(5):943–946, September - October 2005. doi: 10.2514/1.9511.

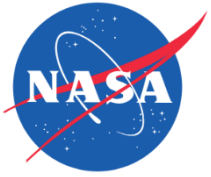


BACKUP SLIDES



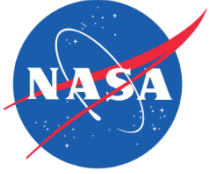
Propellant Estimator Development Road Map

- **Phase I:**
 - Initial development of thermal model
 - Verification made by comparison to other thermal models
 - Provide foundation for Phase II
- **Phase II:**
 - Focus of thesis
 - Refinement of Phase I thermal model
 - Validation/correlation with thermal vacuum test data from MMS spacecraft
- **Phase III:**
 - Calibration of thermal model with flight data
 - Estimations of propellant load on MMS
 - After mid-course orbit change burn
 - At EOL/Decommissioning stage of mission



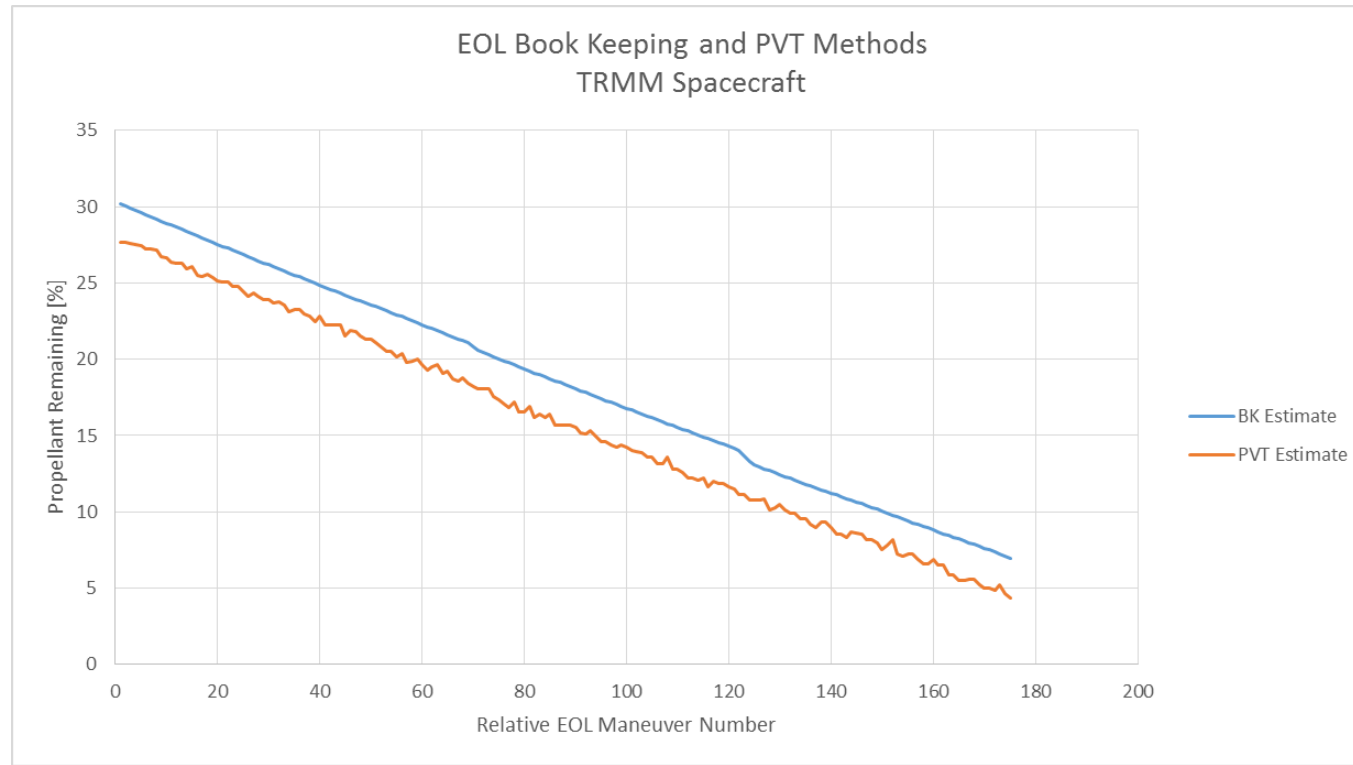
Book Keeping Method Details

- **Use of Thrust Scale Factor (TSF) to decrease Uncertainty**
 - Used on NASA's Tropical Rainfall Measurement Mission
 - TSF acts as learning variable to better predict thruster performance
 - Corrects for differences in thruster performance based on predicted and actual final semi-major axis of spacecraft orbit
- **TSF was found to only marginally improve uncertainties in estimates compared to other book keeping methods, but those uncertainties were still relatively large**

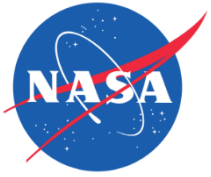


TRMM BKM vs PVT

- BKM and PVT estimates from NASA's TRMM spacecraft
- BK tends to estimate larger amounts of remaining propellant than predictions made by PVT
- Maneuver number shown is relative to start of blowdown operation of TRMM propulsion system



TRMM end of life propellant estimates using BKM and PVT. Maneuver no. relative to beginning of blowdown operation of propulsion system. From Miller, et al [3].



PVT Method: Details

- **PVT relies on 5 key parameters:**
 - Mass of propellant initially loaded
 - Volume & expansion (“stretch”) of propellant tank
 - Tank pressure & temperature
- **More sophisticated models also estimate the leak rate of pressurant gas from system (typically assume worst-case leak rate for whole mission)**
- **Each used to determine propellant mass in following Equations:**

$$V_{prop} = V_T(P, T) - V_g(P, T) \quad (B3)$$

$$PV_g = \left(n_{init} - n_{leak} \right) RT \quad (B4)$$

$$m_p = \rho_p(T) V_{prop} \quad (B5)$$



PVT Method: Pressure Sensitivity

- Lal & Raghunandan performed statistical analysis using Monte Carlo methods to determine how sensitive PVT was to uncertainties in pressure readings
- Branched off of previous work by Chobotov & Purhohit, who developed a method to estimate propellant volume by re-pressurizing a propellant tank [11].
 - Derived following equation to estimate propellant volume:

$$V_L = \left[V_T + (P_u)_f \left(\frac{dV_T}{dP_u} \right) \right] - \left[V_p + (P_p)_f \left(\frac{dV_p}{dP_p} \right) \right] \left(\frac{T_u}{T_p} \right) \left(\frac{\Delta P_p}{\Delta P_u} \right) \quad (B6)$$

Where:

V_L : Estimated mean propellant volume present

V_T : Unstressed propellant tank volume

V_p : Unstressed pressurant tank volume

T_u : Propellant tank temperature

T_p : Pressurant tank temperature

$(P_u)_f$: Propellant tank pressure after re-pressurization

$(P_p)_f$: Pressurant tank pressure after re-pressurization

$\frac{dV_p}{dP_p}$: Pressurant tank stretch coefficients

$\frac{dV_T}{dP_u}$: Propellant tank stretch coefficients

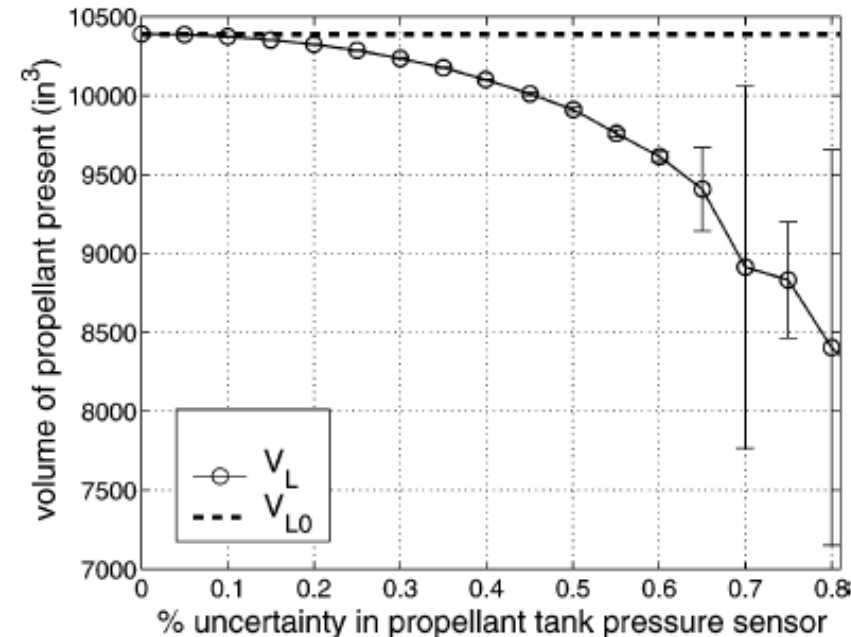
ΔP_p : Pressurant tank pressure decrease due to re-pressurization

ΔP_u : Propellant tank pressure increase due to re-pressurization

- **Sensitivity studies performed by Lal & Raghunandan found**
 - Estimated propellant volume, V_L , was highly sensitive to uncertainties in pressure readings
 - This contributed to high error in subsequent estimates of propellant volume

Parameter	Sensitivity
Propellant tank pressure sensor	125
Pressurant tank pressure sensor	20.2
Propellant tank volume	1.84
Pressurant tank volume	0.852
Pressurant tank temperature sensor	0.854
Propellant tank temperature sensor	0.854
Pressurant tank stretch	0.033
Propellant tank stretch	0.012

Sensitivity of propellant volume estimates to different parameters.
Values from Lal, et al [12].

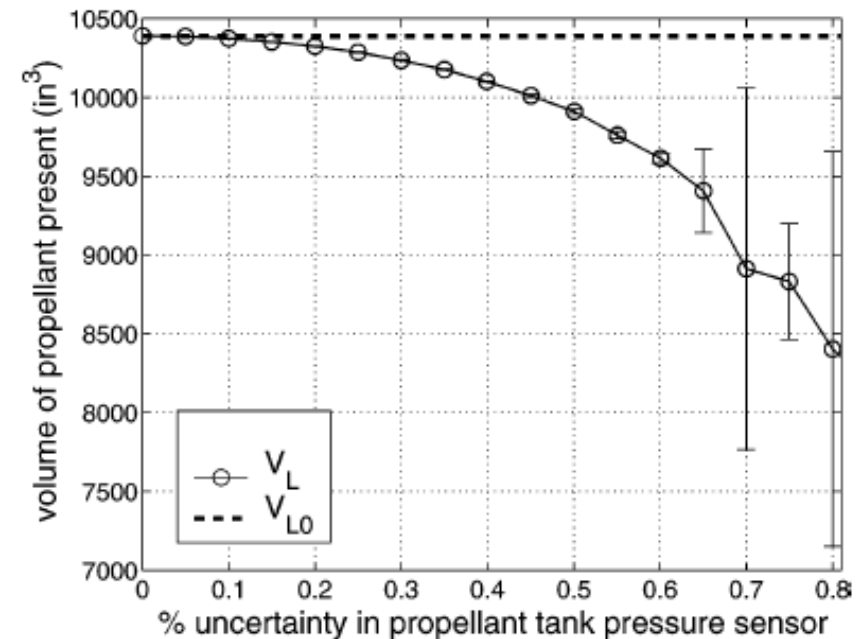


Propellant volume estimate as a function of pressure Transducer uncertainty. From Lal, et al [13].

PVT Method: Pressure Sensitivity

- Deviation of V_L from propellant volume found direct measurement (V_{L0}) caused since:
 - ΔP_U , P_{ui} and P_{uf} are normally distributed about their mean values
 - As uncertainty in pressure measurement increases, term B in V_L equation increases faster than term A
 - This results in estimated propellant volume decreasing away from measured or “true” propellant volume
- High variations (error bars shown) caused because:
 - ΔP_U is typically small (~ 1 psia) and appears in denominator
 - Probability of ΔP_U being zero increases as uncertainty in tank pressure sensor measurement increases

$$V_L = \left[V_T + (P_u)_f \left(\frac{dV_T}{dP_u} \right) \right] - \left[V_p + (P_p)_f \left(\frac{dV_p}{dP_p} \right) \right] \left(\frac{T_u}{T_p} \right) \left(\frac{\Delta P_p}{\Delta P_u} \right)$$

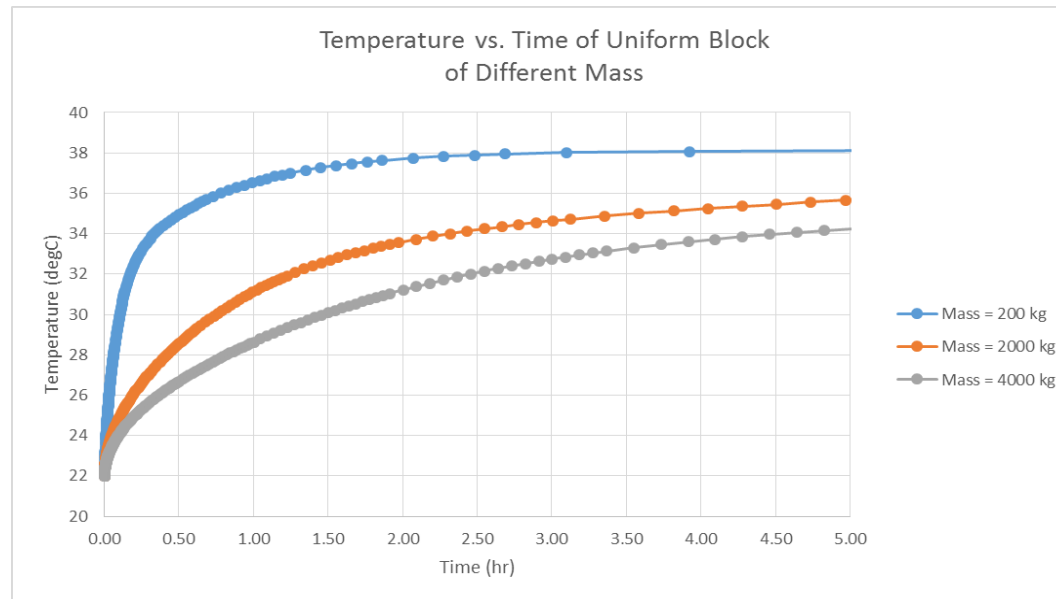


Propellant volume estimate as a function of pressure Transducer uncertainty. From Lal, et al [14].

TCM Theory (cont.)

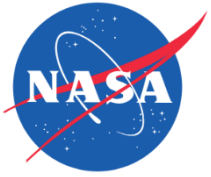
- **Illustrative Example:**

- If specific heat of a material are constant, amount of time to change temperature of a given quantity of matter is a function of the mass of that matter:



- **TCM takes advantage of this fact to estimate propellant load**

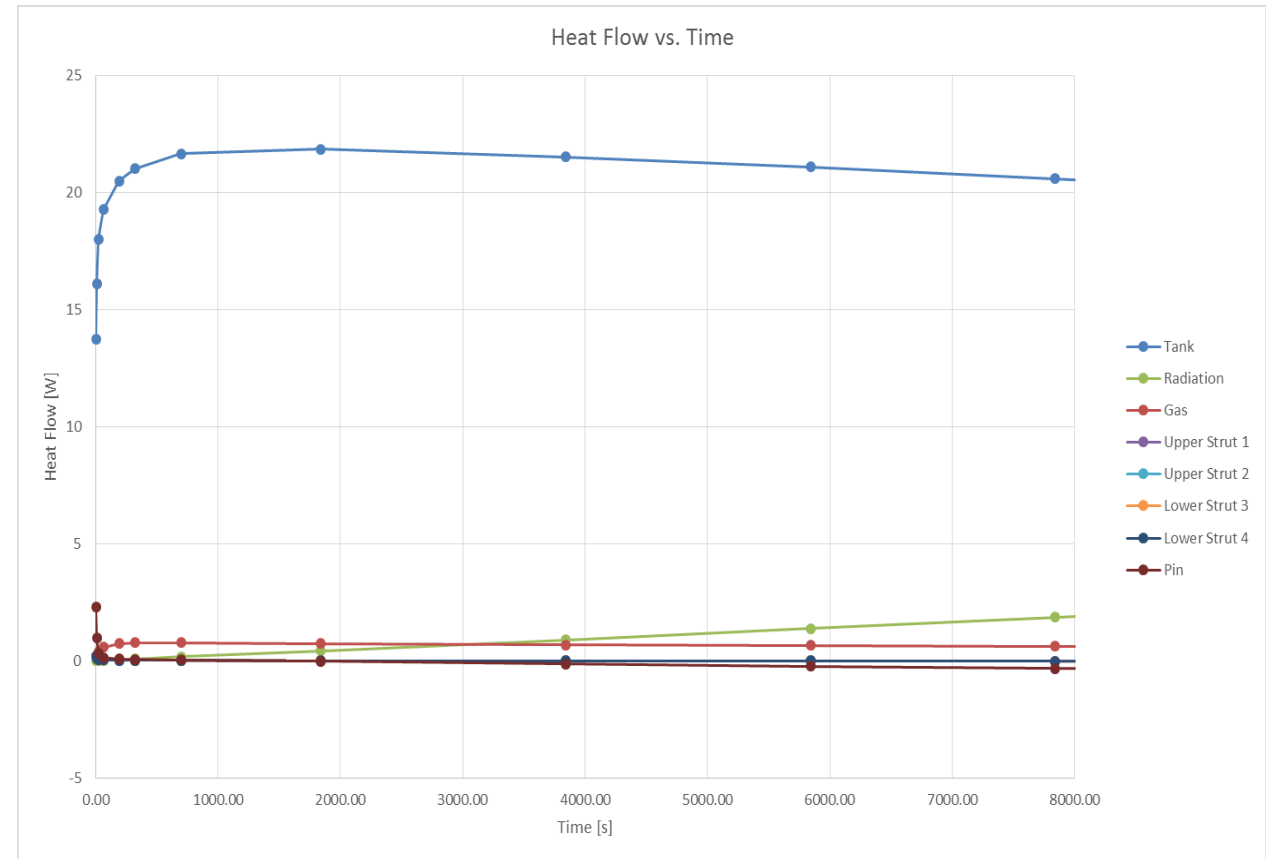
- Propellant tank is heated by turning on tank heaters
- Temperature of the tank is recorded over time
- Recorded T vs. t curves compared to T vs. t curves from thermal model for different propellant loads

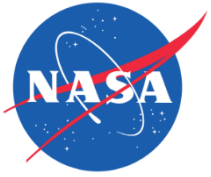


Main Assumptions

- **1): Convection within Gas in tank is neglected**
 - Natural convection does occur in tank (Rayleigh number $> 10e8$), but is not the dominant mode of heat transfer
 - Thermal resistance of gas is much greater than the thermal resistance due to conduction through tank wall
 - Mass of gas is small compared to the mass of the tank wall; therefore the heat capacitance of the gas is smaller than that of the tank wall
 - Causes temperature gradient to form on tank wall more readily than within gas
- **Heat transfer is therefore dominated by conduction through tank wall and other parts, and not through convection within the gas**

- **2): Radiation to environment modeled; surface-to-surface radiation neglected**
 - Radiation was modeled such that the tank radiated to the average environmental temperature of 31°C achieved at TVAC steady-state
 - Emissivity of tank blanket and surfaces were included in model
 - Surface-to-surface radiation is minimized by the thermal design of tank
 - Tank and nearby components covered with blanket with an effective emissivity on order of $1e-4$
 - Parts of tank not blanketed had small surface areas compared to blanketed portions of tank
 - Phase I thermal model revealed:
 - Radiative transfer is small compared to conductive transfer within tank wall after 7000s





Main Assumptions (cont.)

- **3): Perfect bonded contact between interfaces**

- Reflects actual construction of tank

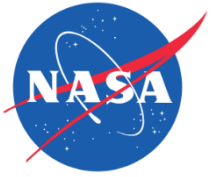
- Tank hardware, struts, tab interfaces, etc. all machined and smooth
- Parts fastened together with multiple fasteners that are torqued
- Thermal hardware is bonded to tank per NASA standards with adhesive that has minimal discontinuities

- Rooted in how ANSYS models thermal contact

- All contacts are defined as “bonded” or “perfect” by default (no conductive losses between connected parts)
- Thermal conductance coefficients (TCC) can be defined at all contacts
- Defining TCC’s at key interfaces was focus of model correlation process
- Majority, however, left as “bonded/perfect”

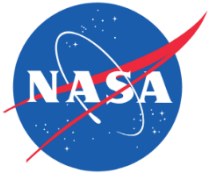
- Not possible to physically characterize all contacts within a real system

- Limited time and money



Assumptions

- 1. Convection within the Nitrogen/Argon mix inside of the tank was neglected. In order for the ANSYS model to close, heat transfer through the gas was modeled as conduction as if the gas were a solid.**
- 2. Radiation is modeled, but surrounding spacecraft enclosure was not**
- 3. A “perfect” bonded contact existed between all interfaces in the model**
- 4. The diaphragm within the tank is not physically modeled, but its mass is accounted for**
- 5. The tank blanket and tape were not physically modeled, but the mass and thermal properties of each were accounted for.**



Assumption: Neglect Convection

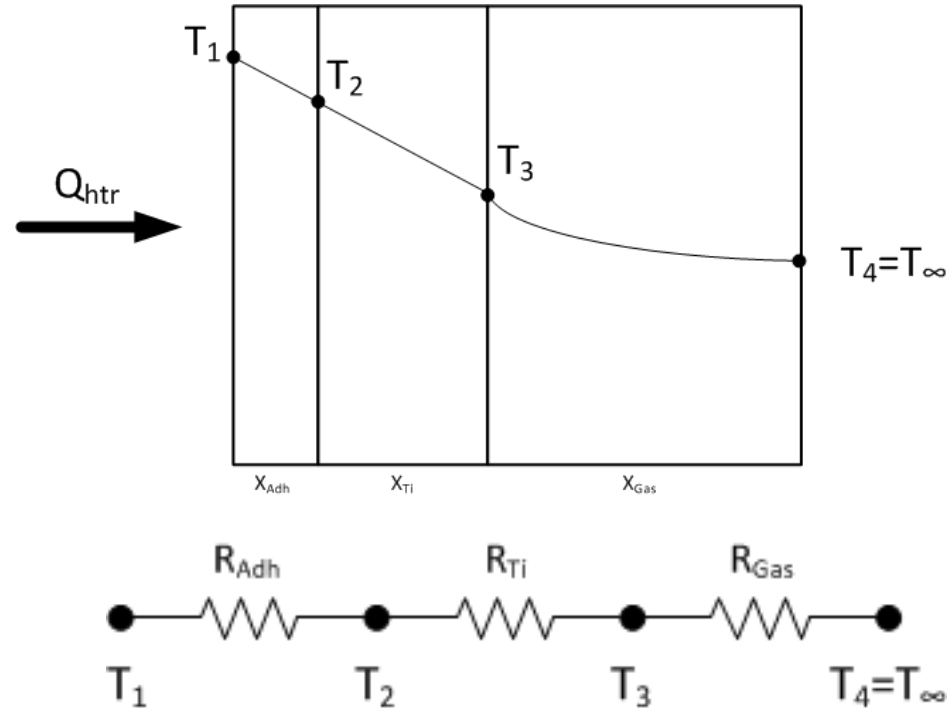
- Rayleigh number was calculated first to determine if heat transfer within gas is primarily conduction or convection:
 - Idealized tank system as vertical flat wall. Reasonable since tank is longer than it is wide

$$Ra = \frac{g\beta(T_w - T_\infty)L^3}{\nu\alpha} \quad (B7)$$

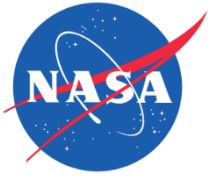
- $T_w = 43^\circ\text{C}$ (set point of over-temp TSTATS)
 - $T_\infty = 31^\circ\text{C}$ (steady-state temperature of tank prior to start of over-temp TSTAT test)
 - $\beta = 1/T_\infty$ (for gases)
 - ν = kinematic viscosity of gas at T_∞
 - α = Thermal diffusivity of gas
 - L = length of wall (height of tank in this case)
- **$Ra = 1.13\text{e}8$. This greater than $10\text{e}8$, so natural convection is occurring in gas within tank**

Assumption: Neglect Convection

- Analyzed thermal resistance of composite system: tank wall, heater adhesive, and pressurant gas



$$q = \frac{T_1 - T_4}{\frac{x_{adh}}{k_{adh}A} + \frac{x_{Ti}}{k_{Ti}A} + \frac{1}{h_{gas}A}} \quad (B8)$$



Assumption: Neglect Convection

- Equation B8 can be written as

$$q = \frac{T_1 - T_4}{R_{adh} + R_{Ti} + R_{gas}} \quad (B9)$$

- To find the convective heat transfer coefficient, the following relations were used:

$$h = \frac{Nuk}{L} \quad (B10)$$

$$Pr = \frac{C_p \mu}{k} \quad (B13)$$

$$Nu = 0.678 Ra^{\frac{1}{4}} \left(\frac{Pr}{0.952 + Pr} \right) \quad (B11) \text{ (Lienhard)}$$

$$Gr_L = \frac{g \beta (T_w - T_\infty) L^3}{\nu^2} \quad (B14)$$

$$Nu = \frac{0.508 Pr^{\frac{1}{2}} Gr^{\frac{1}{4}}}{(0.952 + Pr)^{\frac{1}{4}}} \quad (B12) \text{ (Rohsenhow)}$$



Assumption: Neglect Convection

- Equations B9 – B14 yielded the following:

Quantity	Calculated Value
Grashof Number, Gr	1.7e8
Prandtl Number, Pr	0.663
Nusselt Number via Eq. B11	56.0
Nusselt Number via Eq. B12	41.9
Convection Coefficient, h_{gas} (Nu via Eq. B11)	9.8 W/m² K
Convection Coefficient, h_{gas} (Nu via Eq. B12)	7.4 W/m² K
R_{Gas}	4.6 K/W
$R_{\text{cond}} = R_{\text{Adh}} + R_{\text{Ti}}$	0.03 K/W

- Resulting R_{gas} is 2 orders of magnitude greater than R_{cond}**
 - Heat will tend to flow within the tank wall and heater adhesive more readily than in the gas
 - Flight thermistors (and 1-wire sensors used in the TVAC test) will see temperatures that are representative of wall, rather than gas
 - Convection within gas is not the primary driver affecting the temperature of tank



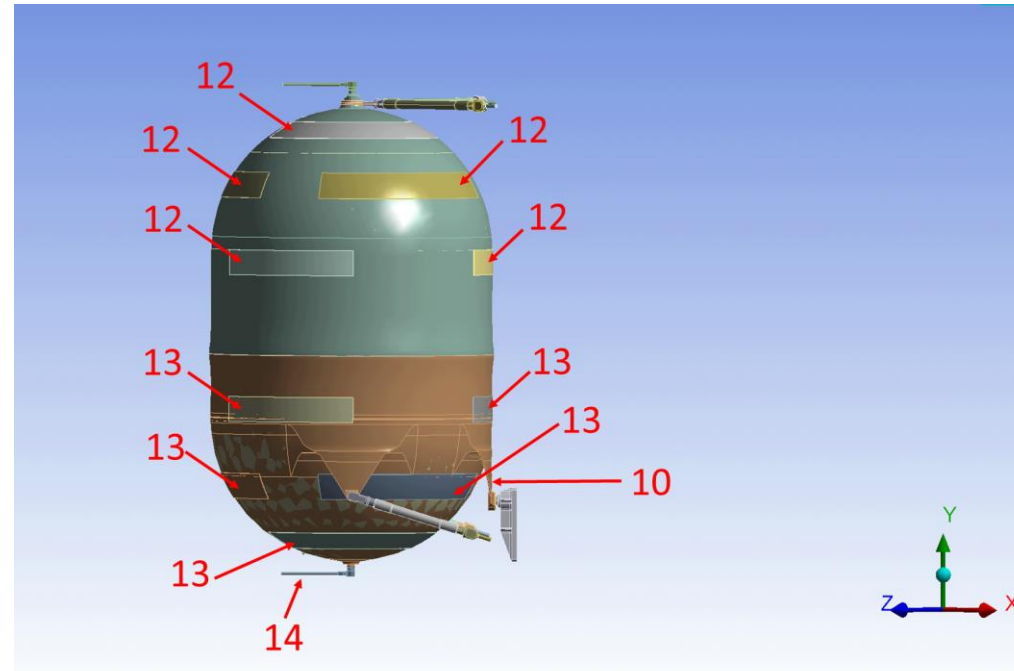
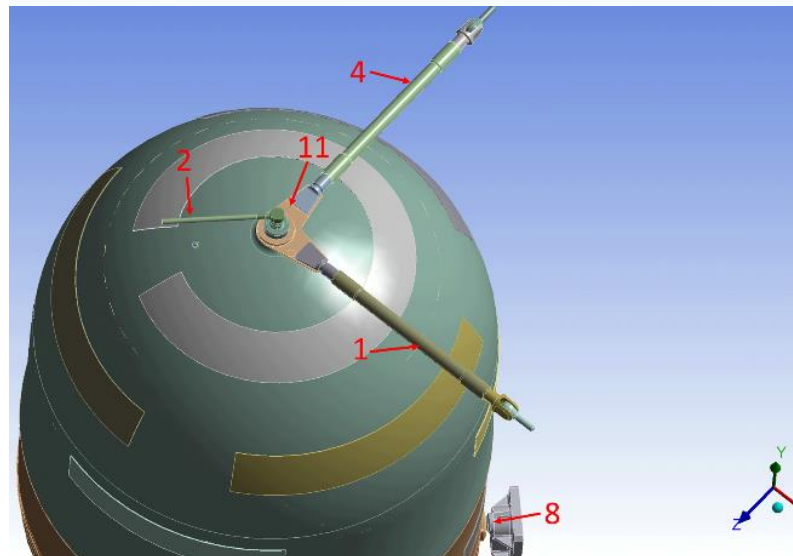
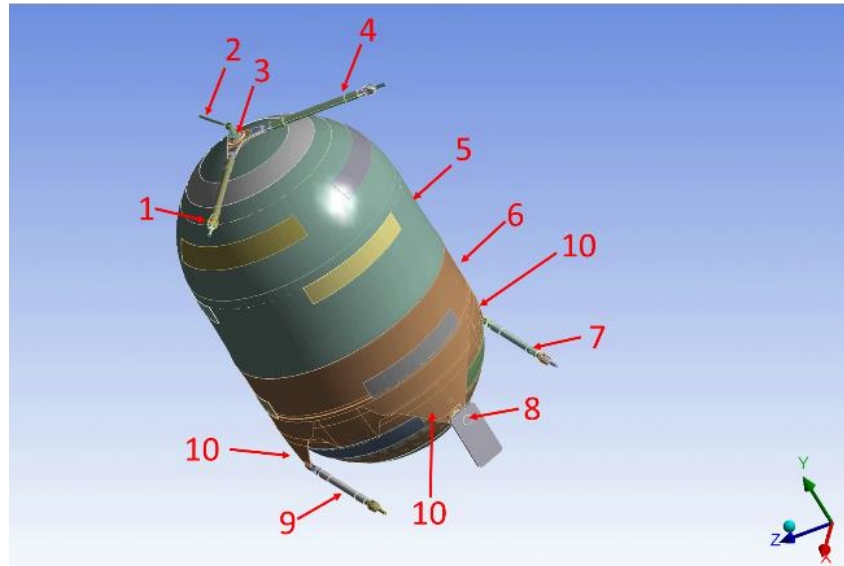
Assumption: Neglect Convection

- Mass of gas and titanium also play a key role in heat transfer
- Can define a ratio of volumetric heat capacity of two materials using Eq. 7

$$\psi = \frac{mc|_{T_i}}{mC_p|_{AR+N_2}} \quad (B15)$$

- $\psi = 9$. Since greater than 1, overall heat transfer for system will be dominated by titanium

Description of Tank System (cont.)



ID	Description	ID	Description
1	Upper Right Strut	8	Axial (Belly Button) Pin (inside of Receiver plate)
2	Gas Inlet Tube	9	Lower Right Strut
3	Gas Side Tank Boss	10	Tank Tab (strut tabs on left/right of tank; belly button tab towards front)
4	Upper Left Strut	11	Boomerang
5	Upper Hemisphere	12	Gas Side Heater
6	Lower Hemisphere	13	Liquid Side Heater
7	Lower Left Strut	14	Liquid Outlet Tube



Mass Smearing

- **Method to account for differences in mass of real part to mass of part in CAD model**
- **Correct mass of parts by changing density of part in ANSYS**
 - Volume of part is fixed via the CAD model
- **Accounts for mass of parts that were distributed around tank or not know explicitly**
 - Tape (distributed around tank)
 - Tank diaphragm, heaters, tank blanket (not known explicitly)
- **Account for small parts removed during de-featuring process**
 - Nuts, bolts, lock-wire, washers, etc.
- **Use mass ratios based upon detailed Flight CAD model of tank to properly distribute part masses**

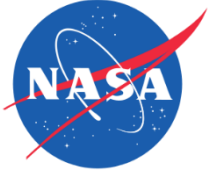
Part: Lower Strut		
Model Volume:	2.98E-05	m ³
Model Initial Density:	5156.05	kg/m ³
Model Initial Mass:	0.15348	kg
Actual Mass:	0.1746	kg
Modified Density:	5866	kg/m ³
New Model Mass:	0.1746	kg/m ³

Mass Ratios used to distribute mass:

$$MR_{Mod} = \frac{M_{CAD,Lower} + X_{mod}}{M_{CAD,Upper} + Y_{mod}} = 0.95 \quad (B16)$$

$$\Delta m = m_{actual} - m_{model} \quad (B17)$$

$$X_{mod} + Y_{mod} = \Delta m \quad (B18)$$

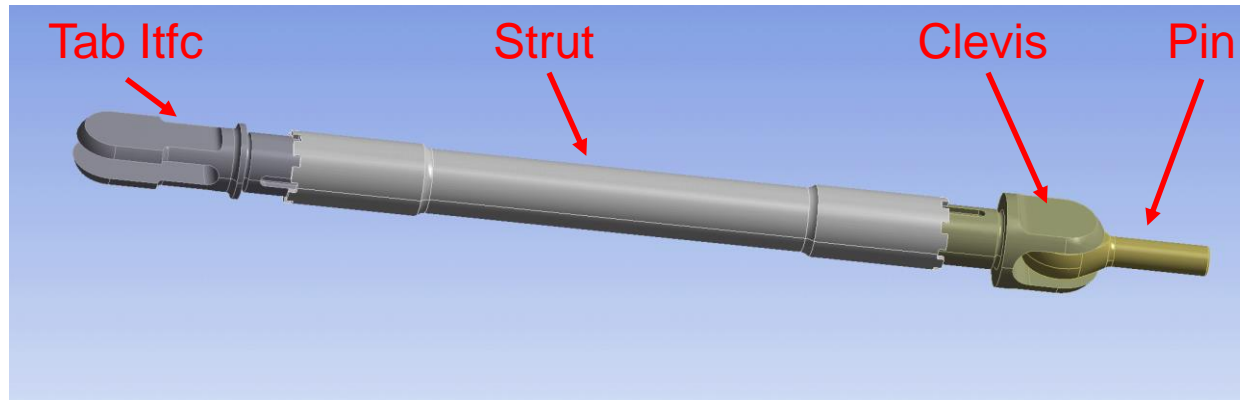


Effective Thermal Conductivity of Grouped Parts

- Solid parts in CAD model grouped to ease correlation process & model losses through a thermal conductance coefficient (TCC)
- ANSYS not allow easy way to apply thermal conductance to a grouped part
 - TCC only applied to specific contact
 - Have to change TCC at every contact within grouped part, which becomes cumbersome in a large model
 - Specific information about TCC at every contact may or cannot be known
- Alleviate problem by defining groups of parts that share thermal properties based upon mass fraction of parts within the group
- Properties of grouped part are made into a new “material” which is assigned to the grouped part
- Thermal conductance of part changed by modifying thermal conductivity of grouped part since:
 - Cross sectional area of part is fixed and based upon the CAD model of the part
 - Length of part is fixed and based upon the CAD model of the part

Effective Thermal Conductivity of Grouped Parts

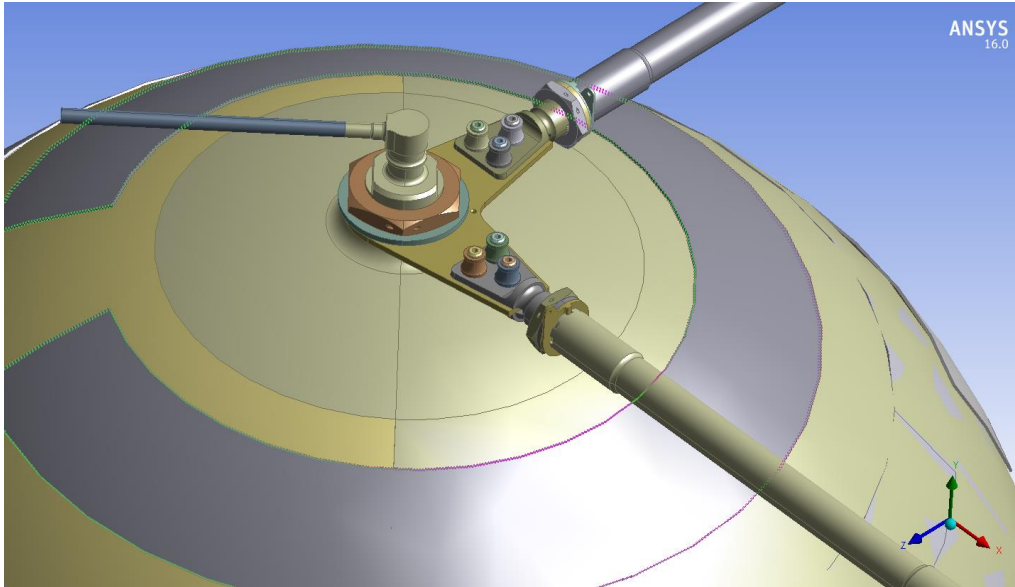
- Example: Tank Strut



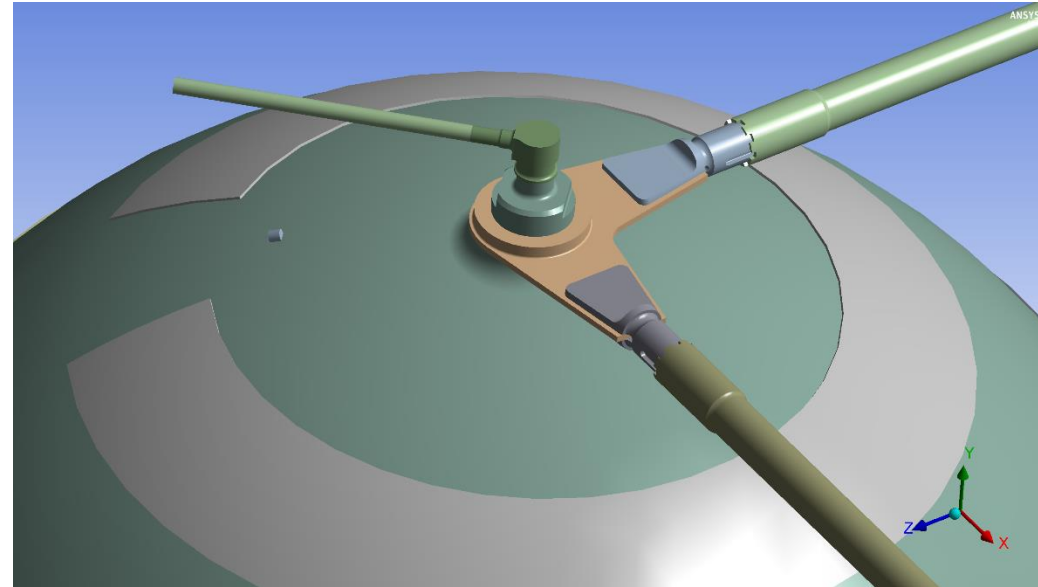
Sub Material	Mass Fraction	Thermal Conductivity (W/m K)	Specific Heat (J/kg K)
17-4 PH: Pin	0.21	10.46	460.50
6-4 Ti: Tab Itfc	0.24	7.20	554.3
6-4 Ti: Clevis	0.22	7.20	554.3
3-2.5 Ti: Strut	0.34	7.20	554.3
	Mix:	7.91	534.66

Model De-featuring

- Refers to removing extraneous parts from model that do not play a large role in heat transfer
- If left in, would greatly increase size and complexity of mesh
- Examples of parts removed:
 - Small sensors, bolts, nuts washers
 - Fill bolt holes, correct CAD importation errors such as slivers and small faces

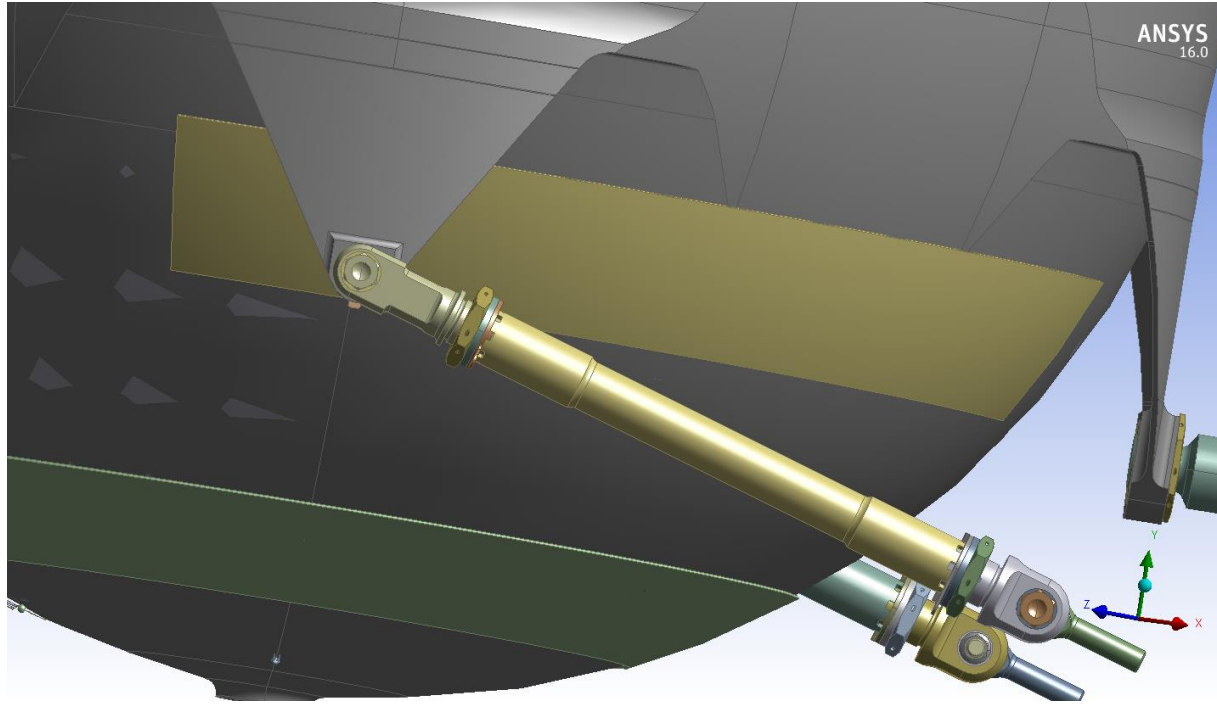


Before

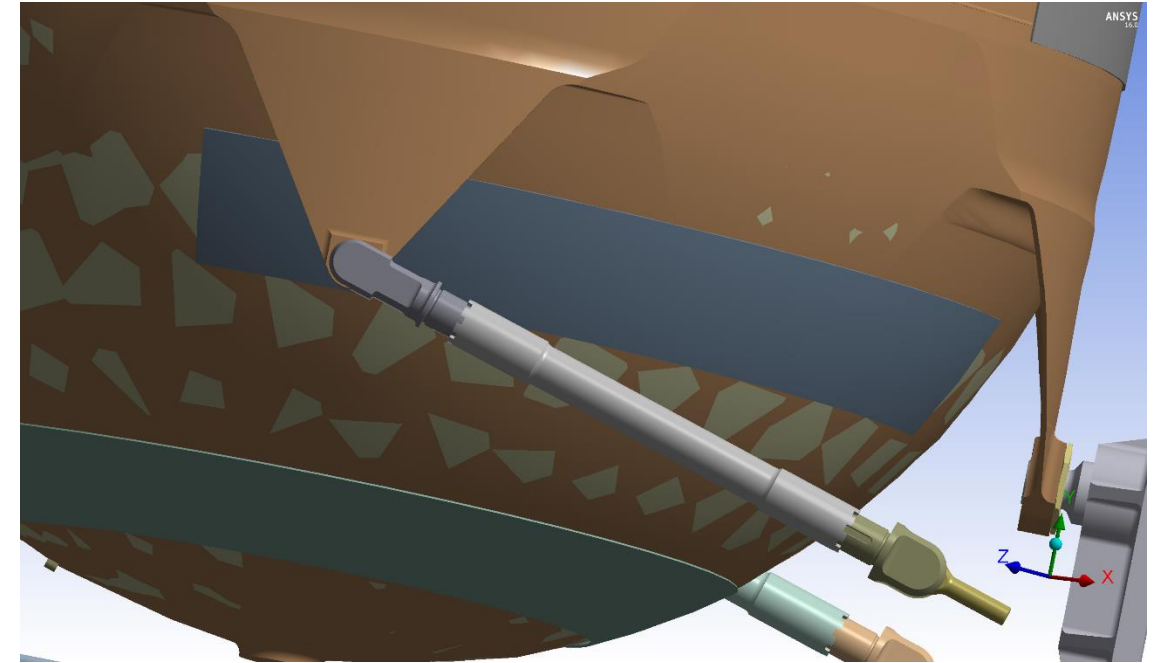


After

Model De-featuring (cont.)



Before



After



Thermal Error

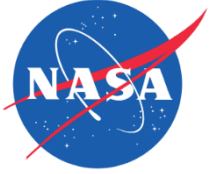
- Thermal error provides a *relative* measure of difference in flux between elements
- Difference calculated by subtracting thermal flux vector in each node from the nodal average thermal flux. (Eq. B19)
- Error per element is found by numerically integrating all of the nodal flux differences and then summing them (Eq. B20 – B21)

$$\Delta \mathbf{q} = \mathbf{q}^a - \mathbf{q}^i \quad (\text{B19})$$

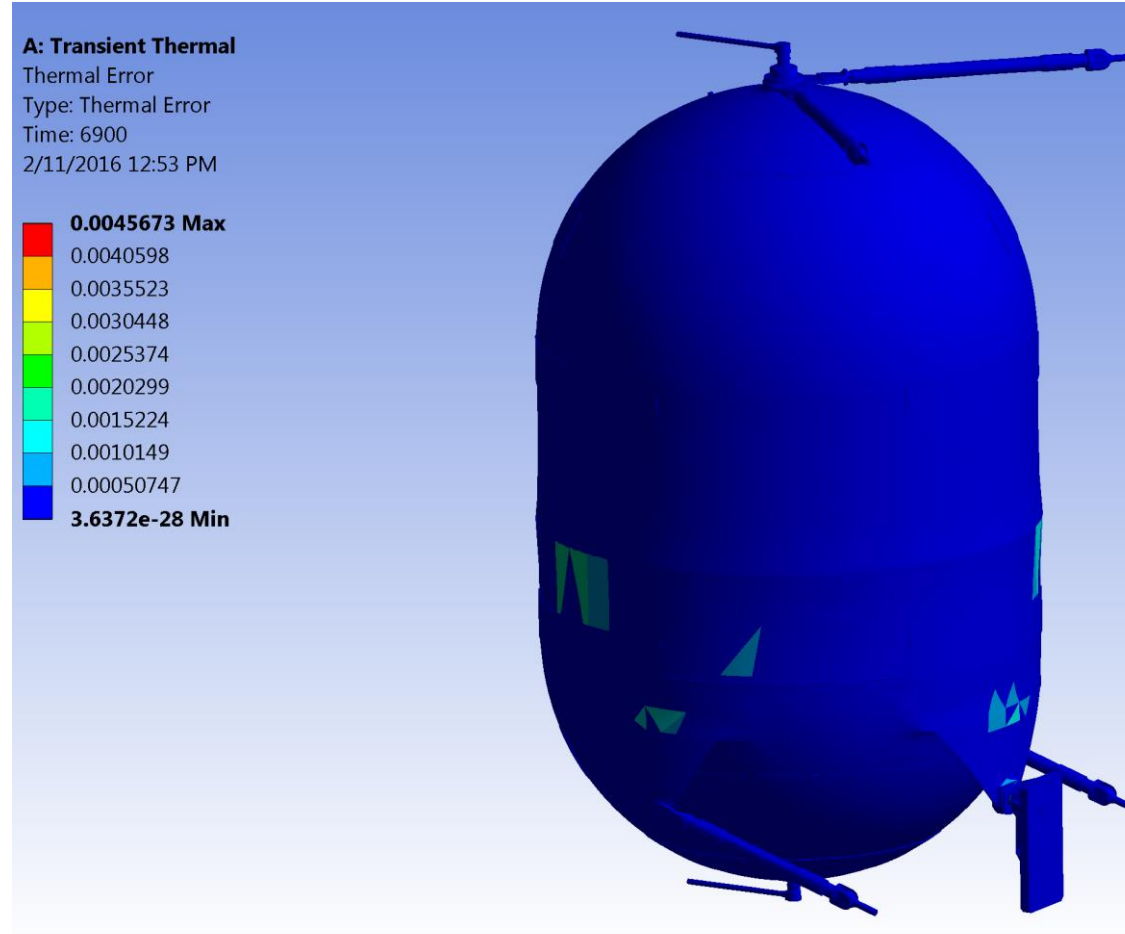
$$e_i \propto \int \Delta \mathbf{q} \, dV_{elem} \quad (\text{B20})$$

$$e = \sum_i^N e_i \quad (\text{B21})$$

- More nodes model has, the smaller e_i is.
- Relative measure since only compares fluxes from element to element, and not compare all elements simultaneously
- ANSYS recommends the use of thermal error to determine which parts of the model need mesh refinement



Thermal Error





Correlation Study Results

- **Final Configuration:**
 - Used to generate correlated model results

Location	TCC	Location	k Multiplier
Upper Right Strut at Pin	150	Upper Hemisphere k Mult	1.5x
Upper Left Strut at Pin	150	Lower Hemisphere k Mult	2.0x
Lower Right Strut at Tab	20	Upper Right Strut k Mult	2.5x
Lower Left Strut at Tab	20	Upper Left Strut k Mult	1.0x
Upper Right at Boomerang	Baseline	Lower Right Strut k Mult	2.0x
Upper Left at Boomerang	Baseline	Lower Left Strut k Mult	1.0x
		Gas Inlet & Outlet Tube	1.0x
		Axial pin	1.0x



Uncertainty Analysis Details

- Uncertainty in Heat Flux (function of resistance and circuit current)

Heat flux from heater circuit:

$$q_g = \frac{(i_c R_c)^2}{R_g A} \quad (\text{B22})$$

$$R_{circ} = \frac{R_L R_g}{R_L + R_g} \quad (\text{B23})$$

Combining Eq. B13 - B14:

$$q_g = \frac{i_c^2 R_g R_L^2}{(R_L + R_g)^2 A} \quad (\text{B24})$$

Uncertainty in heater circuit heat flux:

$$\frac{U_q}{q_g} = \sqrt{\left(\frac{i_c}{q_g} \frac{\partial q_g}{\partial i_c}\right)^2 \left(\frac{U_{i_c}}{i_c}\right)^2 + \left(\frac{R_g}{q_g} \frac{\partial q_g}{\partial R_g}\right)^2 \left(\frac{U_{R_g}}{R_g}\right)^2 + \left(\frac{R_L}{q_g} \frac{\partial q_g}{\partial R_L}\right)^2 \left(\frac{U_{R_L}}{R_L}\right)^2} \quad (\text{B25})$$

$$\frac{U_q}{q_g} = \sqrt{4 \left(\frac{U_{i_c}}{i_c}\right)^2 + \left(\frac{R_L - R_g}{R_g + R_L}\right)^2 \left(\frac{U_{R_g}}{R_g}\right)^2 + \left(\frac{2R_g}{R_g + R_L}\right)^2 \left(\frac{U_{R_L}}{R_L}\right)^2}$$

Where:

$$U_{R_g} = U_{R_L} = \frac{1}{N \left(\frac{1}{\Delta R_{wrst}}\right)}$$

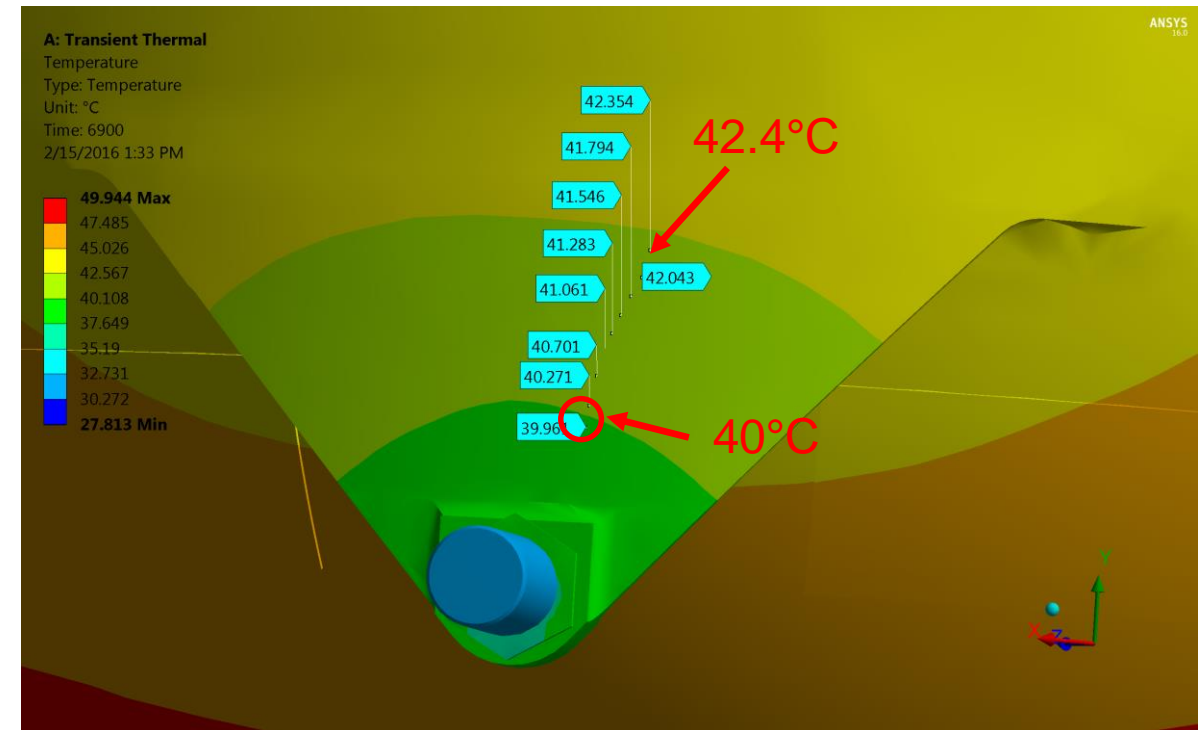
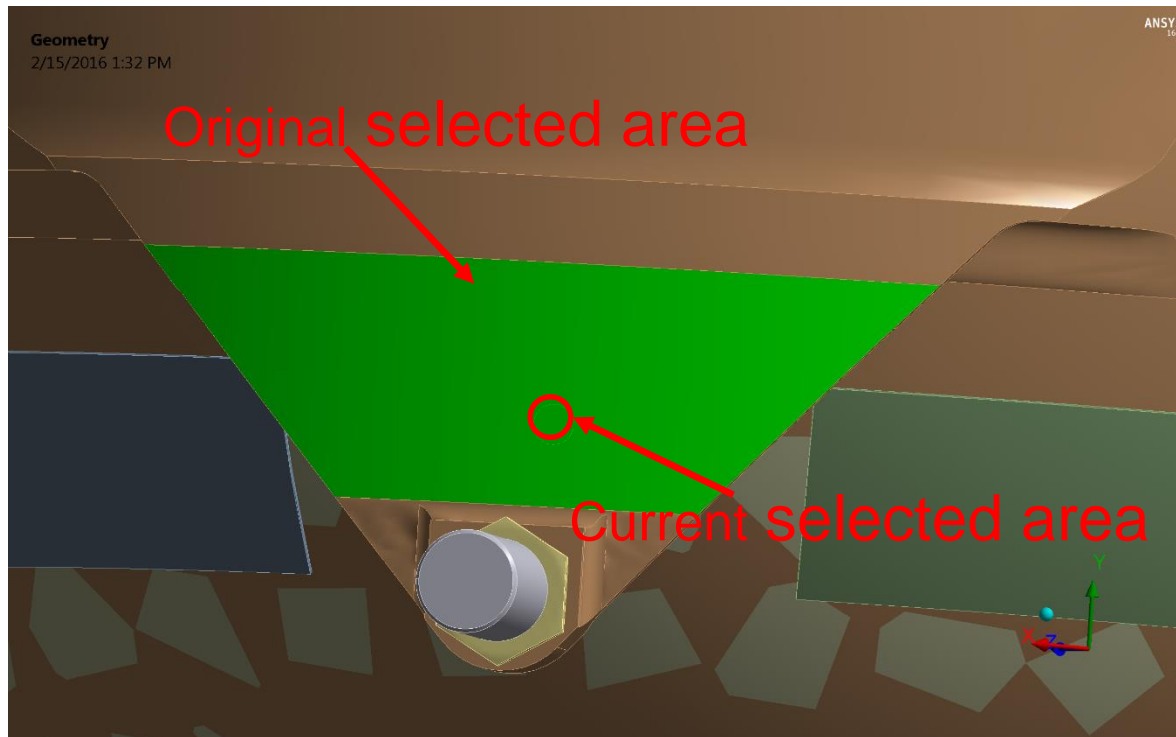
$$N = 7$$

$$\Delta R_{wrst} = 2.5\Omega$$

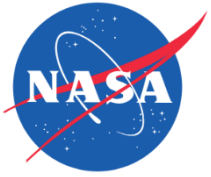
$$U_{i_c} = 2\%FS + e_{bit} = 0.041$$

Key Lesson Learned

- Understand how software queries results from model
 - Temperature probe tool returns maximum of selected area, not average temperature



- Add complexity incrementally, rather than remove complexity



Key Lessons Learned

- **Reduce complexity of solid model**
 - Results in a less complicated correlation process
 - Faster solve times
 - More control can be achieved by adding complexity, rather than working backwards to reduce complexity
- **Document changes to model and corresponding results in one place**
 - Changes were all documented, but initially organization was not good
 - Compilation of changes was done later, which cost time